Structures and Materials Research Report No, 98-1
FINAL PROJECT REPORT

July 1998

UF Project No. 4910 45 04 569 12
State Job No. 99700-1502-010
Contract No. BA585
WPI No. 0151697

DEFLECTION CALCULATION MODEL FOR STRUCTURES WITH ANNULAR BASE PLATES

Ronald A. Cook
Marc I. Hoit
Sara B. Nieporent

Department of Civil Engineering
College of Engineering
UNIVERSITY OF FLORIDA
Gainesville

Engineering and Industrial Experiment Station

Technical Report Documentation Page

1. Report No.	2. Government Accession No.	3. Recipient's Catalog No.
WPI 0151697		

4. Title and Subtitle

Deflection Calculation Model for Structures with Annular Base Plates

5. Report Date: July 1998

6. Performing Organization Code:

8. Performing Organization Report No.: 4910 45 04 569 12

7. Author(s)

R.A. Cook, M. I. Hoit, S. B. Nieporent

9. Performing Organization Name and Address

University of Florida
Department of Civil Engineering
345 Weil Hall / P.O. Box 116580
Gainesville, FL 32611-6580

10. Work Unit No. (TRAIS): 99700-1502-010

11. Contract or Grant No.: BA 585

12. Sponsoring Agency Name and Address

Florida Department of Transportation
Research Management Center
605 Suwannee Street, MS 30
Tallahassee, FL 32301-8064

13. Type of Report and Period Covered: Final Report 9/10/96 - 7/10/98

14. Sponsoring Agency Code: 99700-1502-010

15. Supplementary Notes

Prepared in cooperation with the Federal Highway Administration

16. Abstract

The deflections of mast arm and light pole structures are typically calculated by assuming the structure to be fixed at the base. However, additional rotation from the base plate and anchor bolts has been found to increase the overall deflection. The purpose of this study was to evaluate the contribution of the base plate and anchor bolts to the overall deflection (rotation) of a typical mast arm and light pole.

A finite element model of the base plate system was first used to predict the deflection and overall rotation. To verify its accuracy, the results of the finite element model were compared to lab tests in which a tubular member was welded to an annular base plate that was connected to a foundation with anchor bolts. The finite element model was then used to calculate the deflections and rotations of typical Florida Department of Transportation (FDOT) base plate systems.

Based on the results of the finite element study, a design equation was developed using the virtual work method. The design equation was calibrated to the results of the finite element analysis. The resulting design equation is appropriate for calculating the rotation of annular base plates for typical FDOT mast arm and light pole structures.

17. Key Words	18. Distribution Statement
Annular Base Plates, Base Plates, Mast Arms, Traffic Signal Supports, Deflections, Anchor Bolts	No restrictions. This document is available to the public through the National Technical Information Service, Springfield, VA, 22161

19. Security Classif. (of this report)	20. Security Classif. (of this page)	21. No. of Pages	22. Price
Unclassified	Unclassified	99	

Form DOT F 1700.7 (8-72)

DISCLAIMER

"The opinions, findings and conclusions expressed in this publication are those of the authors and not necessarily those of the Florida Department of Transportation or the U.S. Department of Transportation.

Prepared in cooperation with the State of Florida Department of Transportation and the U.S. Department of Transportation."

TECHNICAL SUMMARY

The deflections of mast arm and light pole structures are typically calculated by assuming the structure to be fixed at the base. However, additional rotation from the base plate and anchor bolts has been found to increase the overall deflection. The purpose of this study was to evaluate the contribution of the base plate and anchor bolts to the overall deflection (rotation) of a typical mast arm and light pole.

A finite element model of the base plate system was first used to predict the deflection and overall rotation. To verify its accuracy, the results of the finite element model were compared to lab tests in which a tubular member was welded to an annular base plate that was connected to a foundation with anchor bolts. The finite element model was then used to calculate the deflections and rotations of typical Florida Department of Transportation (FDOT) base plate systems.

Based on the results of the finite element study, a design equation was developed using the virtual work method. The design equation was calibrated to the results of the finite element analysis. The resulting design equation is appropriate for calculating the rotation of annular base plates for typical FDOT mast arm and light pole structures.

DEFLECTION CALCULATION MODEL FOR STRUCTURES WITH ANNULAR BASE PLATES

WPI No. 0510697
State Job No. 99700-1502-010
Contract No. BA585
UF No. 4910 45 04 569 12

Principal Investigator: R. A. Cook

Graduate Research Assistant: S. B. Nieporent

FDOT Technical Coordinator M. H. Ansley

Engineering and Industrial Experiment Station
Department of Civil Engineering
University of Florida
Gainesville, Florida

TABLE OF CONTENTS

page

CHAPTERS

CHAPTER 1
INTRODUCTION

1.1 General

Annular base plates, combined with anchor bolts, are typically used to connect tubular high-mast poles, roadway light poles, and traffic mast arms to a concrete foundation. These connections are subjected to a fairly high bending moment with axial compression loading. Some research has been performed on base plates subjected to axial compression with and without small eccentricities. However, there has been little research done on the behavior of annular base plates dominated by moment.

The Florida Department of Transportation (FDOT) uses the annular base plates in the construction of the tubular high-mast poles, roadway light poles, and traffic mast arms. Rational design procedures exist for sizing the tubular member as well as the weld connecting the member and the annular base plate. Additionally, design procedures exist for determining the embedment requirements for the anchor bolts. Previous research has also been performed for FDOT by the University of Florida (Cook et al., 1995) to develop a rational method for determining the serviceability and strength requirements of the base plate. This research demonstrated that a significantly greater deflection was occurring than predicted based on flexural deformation of the light pole or mast arm.

1.2 Objective

The overall objective of this study was to develop a design equation for calculating deflections associated with annular base plate connections, including the contribution from both the annular plate and anchor bolts.

1.3 Scope

This project was divided into five parts:

1) Selection of the computer code and model,
2) Generation of the computer model,
3) Verification of the computer model,
4) Parameter study of various base plate configurations, and
5) Development of a design equation for calculating deflections.

The first part of the project dealt with determining which computer code to use for the generation of the computer model. Matlab was chosen because it provided a simple method of writing computer code and compiling the necessary information. SSTAN (Hoit, 1995) was then chosen as the finite element program since it provided an accurate, efficient, cost effective mean of analysis.

In the second part of the project, a pre-processor was developed. The pre-processor could generate a complete finite element input file of the annular base plate system with minimal input by the user. The resulting input file could then be used with SSTAN (Hoit, 1995) to generate information such as stresses, deflections, and moments.

The third part consisted of analyzing base plate configurations from the previous experimental research (Cook et al., 1995) using the finite element program. Results were compared to those of the previous experimental tests to verify the model.

The computer model was then used to extrapolate the results to larger member sizes, such as those used in typical FDOT installation.

Finally, a design equation was developed to predict rotations based on the finite element analysis coupled with verification from the experimental results.

CHAPTER 2
BACKGROUND

2.1 Introduction

Minimal experimentation has been performed on rectangular steel base plates subjected to large bending moment (Cook et al., 1989). Some work has been conducted on rectangular base plates considering a column-type connection containing either a concentric axial load or an axial load with a small eccentricity. A design equation based on this work is reported in the American Institute of Steel Construction (AISC) Columns Design Manual (DeWolf, 1991). With the exception of a study by Cook et al. (1995), there appears to be no previous work reported on annular base plate connections subjected to large bending moment.

The experimentation performed by Cook et al. (1995) for the FDOT developed a design standard for the serviceability and strength of annular base plates subjected to large moments. In this study, it was determined that the measured deflection of the base plate system, including the pole, base plate, and anchor bolts, exceeded the expected cantilever beam deflection by approximately three times. The study reported in this thesis was a continuation of the previous research (Cook et al., 1995) in order to develop a methodology for determining the deflection of annular base plates loaded primarily by moment.

2.2 Related Theoretical and Empirical Solutions

2.2.1 Timoshenko's Equation for Plate Bending

Timoshenko and Woinowsky-Krieger (1969) developed equation (2-1) for the deflection of a circular plate subjected to moment, simply supported around the outer edge. The central portion of the plate, with radius b, was considered to be absolutely rigid:

$$\omega = \frac{-Ma}{8\pi D[(3+\nu)+(1-\nu)\beta^4]}\{-[(1+\nu)+(1-\nu)\beta^2]\rho^3+(1+\nu)(1-\beta^2)^2\rho + 2[(3+\nu)+(1-\nu)\beta^4]\rho\log\rho-\beta^2[(1+\nu)\beta^2-(3+\nu)]\rho^{-1}\}\cos\theta \quad (2\text{-}1)$$

where,

M = applied moment

a = distance from center of plate to support

D = plate rigidity = $Et^3/12(1-\nu^2)$

ν = Poisson's ratio

t = thickness of plate

E = modulus of elasticity

β = b/a

b = radius of central rigid portion of plate

a = radius of supports

ρ = x/a

x = radius to point evaluating for deflection

θ = polar coordinate for direction of moment

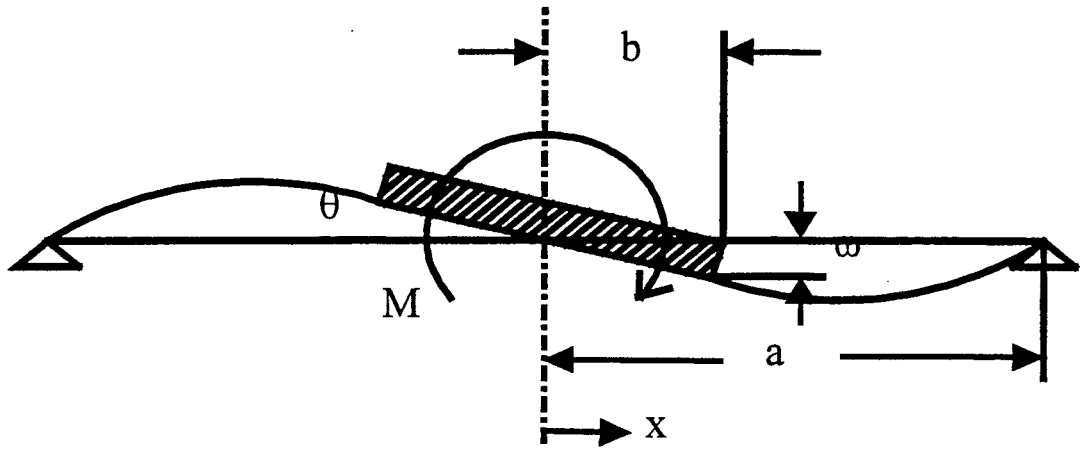

Figure 2.1 Notation Used for Timoshenko's Circular Plate (1969)

2.2.2 Formulas for Circular Plates of Constant Thickness

In Roark's Formulas for Stress and Strain (Young, 1989), a formula has been presented for a central couple on an annular plate with a simple supported outer edge. The equation for the radial slope of the plate is shown below.

$$\theta = \frac{cM}{Et^3} \tag{2-2}$$

The coefficient, c, used in formula (2-2) is based on the ratio of r_p/r_b, where r_p is the radius of the pipe and r_b is the distance from the center of the pipe to the center of the bolt. This formula limits the shear and normal stress occurring in the base plate to the following maximum values:

$$\tau_{max} = \frac{\lambda M}{r_b t^2} \tag{2-3}$$

$$\sigma_{max} = \frac{\gamma M}{r_b t^2} \tag{2-4}$$

The maximum shear and normal stress can be found at the pipe-plate interface.

2.2.3 Formula for Deflection Based on Research by Cook et al. (1995)

According to Cook et al. (1995), the total rotation of a base plate system was attributed to the combination of three factors given in Equation (2-5).

$$\theta = \theta_{bolt} + \theta_{plate} + \theta_{weld} \tag{2-5}$$

A portion of the rotation of the system comes from the anchor bolts. When the system is loaded, the compression bolts shorten while the tension bolts elongate, causing a rigid body rotation of the base plate. The equation for rotation due to the deformation of the anchor group in the elastic range was based on the theoretical equation for axial flexibility of a single bolt. The study determined a factor of 1.5 should be multiplied by the theoretical flexibility to get the rotation due to the bolts. The 1.5 factor accounted for the localized crushing of the concrete around the embedded head of the anchor (in tension and compression) due to the high compressive stress (Collins et al., 1989). The equation calculating rotation due to the anchor bolts was based on the formula for deformation:

$$\theta_{bolt} = \frac{1.5 M L_b}{s_g A_b E_b r_b} \tag{2-6}$$

M = applied moment on the anchor bolt

L_b = length of bolt under tension or compression

s_g = section modulus of the bolt group about the axis of moment application per unit area

$$s_g = \frac{\sum y_b^2}{y_{max}} \tag{2-7}$$

y_b = distance from the centroid of the bolt group to a particular bolt

y_{max} = distance from the centroid of the bolt group to the outermost bolt

A_b = cross-sectional area of the bolt

E_b = modulus of elasticity of the bolt

r_b = distance from the center of the plate to the center of the outermost bolt

Additionally, the plate and weld contributed to the rotation. The rotation due to the plate and weld are closely tied to each other since the flexibility of the welded joint directly effects the overall flexibility of the base plate. The equation found by Cook et al. (1995) was based on Timoshenko's equation (2-1) which was derived for a circular plate with the central portion, where the tubular member is connected, considered absolutely rigid.

$$\theta_{plate+weld} = \left(\frac{0.7M}{Et^3\alpha}\right)\left[1-\alpha^2\right] \tag{2-8}$$

where,

M = applied moment

t = thickness of base plate

E = modulus of elasticity

$\alpha = r_p/r_b$

r_p = outside radius of pipe

r_b = distance from center of plate to center of bolt

It was also interesting to note the similarity of equation (2-8) to Roark's equation (2-2). For typical FDOT ranges, α varied approximately from 0.7 to 0.85. The coefficient, c, from equation (2-2) had a value of 0.528 when α was 0.7 and 0.236 for an α of 0.85. Based on the ranges of α, the ratio from equation (2-8) can be compared to the value, c, by simplifying it into equation (2-9).

$$c = \frac{0.7}{\alpha}\left(1 - \alpha^2\right) \tag{2-9}$$

This ratio varied from 0.51 when α was 0.7 to 0.229 when α was equal to 0.85. However, this equation still underestimated the rotation of the system.

2.3 Effect of Shear on Base Plates

According to Ugural (1981), shear generally is neglected when calculating the bending of plates since the contribution to the overall deflection is usually slight. However, for a circular plate that has a large thickness compared to its radius, shear must be considered. Young (1989) stated that when circular plates have large openings, the deflection due to shear might constitute a considerable portion of the total deflection. Whal and Lobo (1933) suggest that for plates with simply supported edges, shear should be evaluated when the thickness is greater than one-third the difference in inner and outer diameters. To account for this effect, Ugural (1981) suggests increasing the deflection due to the pipe by the following plate slenderness factor:

$$\Delta'_{plate} = \left(1 + \frac{3}{2}\left(\frac{t}{r_\Delta}\right)^2\right)\Delta_{plate} \qquad (2\text{-}10)$$

where, $r_\Delta = r_b - r_p$.

2.4 Deflection Limitations

The AASHTO Standard Specifications (1994) provide the following guideline for the deflection of cantilever supports for luminaires, traffic signals, and signs subjected to moment load applications: "Deflection can be expressed in terms of a slope deviation or an angular rotation. The commonly used, maximum theoretical slope deviation is 0.009 m (0.35 inches) in 0.305 m (12 inches)." Additionally, a limit of L/50, where L is the structure length, was recommended for a maximum deflection (Cook et al., 1995).

CHAPTER 3
DEVELOPMENT OF COMPUTER MODEL

The base plate system was modeled to evaluate the rotational effects of a typical FDOT mast arm. Rotation of this system resulted from plate bending as well as the elongation and shortening of the anchor bolts. A typical installation consists of either a very tall light pole or a cantilevered mast arm. By modeling a short segment of pipe, the annular plate, and the anchor bolts, the overall rotation from the plate and anchor bolts could be determined.

The computer model was generated to produce the same effects that occurred in the laboratory tests performed by Cook et al. (1995). The rotation of the base plate system (base plate and anchor bolts) was determined by the following equation:

$$\theta_{plate} = \frac{\left(\Delta_{total} - \Delta_{pipe}\right)}{L_{pipe}} \tag{3-1}$$

The total deflection, Δ_{total}, was the deflection at the top of the pipe, and Δ_{pipe} was the cantilevered deflection of the pipe. The pipe's length was L_{pipe}. The rotation, θ_{plate}, represents the overall rotation due to the base plate and anchor bolts.

3.1 Anchor Bolt Modeling

A working model of the base plate was initially developed using elements creating a circle-like pattern to model the bolts. Figure 3.1 shows a typical pattern. The

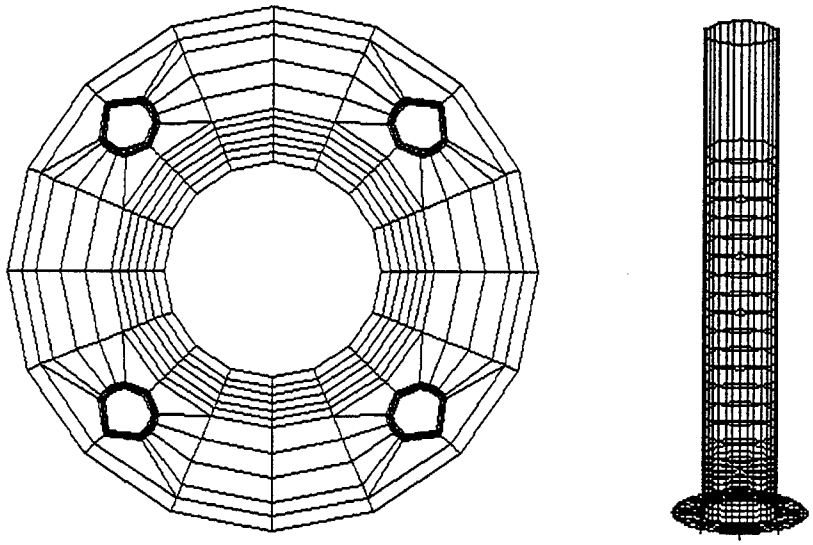

Figure 3.1 Base Plate and Pipe Model

circular base plate was developed using symmetry. A pie shaped portion of the base plate was first developed with the bolt hole as the center, as shown in Figure 3.5. The pie shape was then regenerated a number of times equal to the number of bolts, thus completing the entire base plate.

The bolts were then modeled using a series of beams to produce a response equivalent to the flexural and axial deformations occurring in the bolts and plate. The bolts behaved analogously to a spring. The bolt model contained beam elements that connected the nodes that model the edges of the bolt to the node in the center of each bolt as shown in Figures 3.2 and 3.3. Those radial beam elements were made to be very rigid.

A beam element also connected the center node to a node at the point where the bolt entered the concrete. The latter beam modeled the properties of the actual bolt, containing the area and moment of inertia necessary to correctly model the axial and flexural stiffness of the bolt. It is important to note that since the actual bolt was much longer then the modeled bolt, an adjusted bolt area was used to obtain the correct axial stiffness. This is further explained in section 3.4.

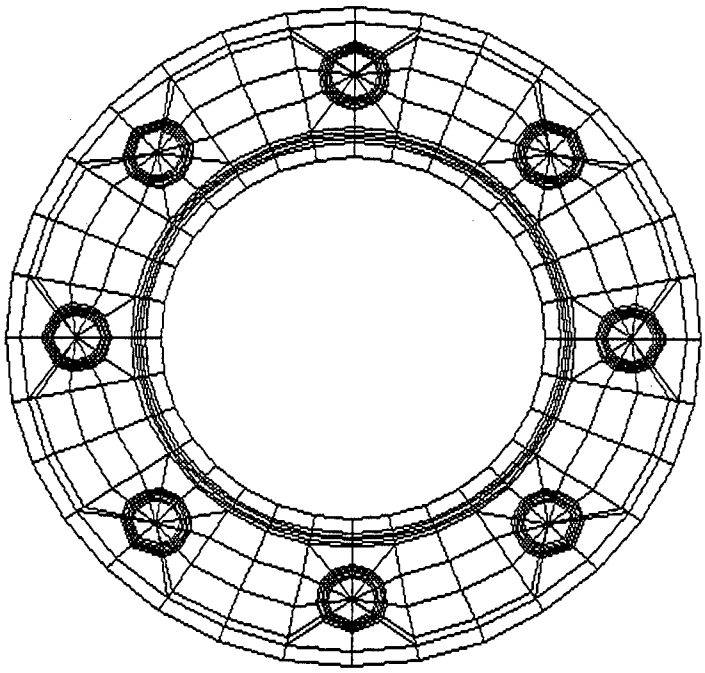

Figure 3.2 Plan View of a Base Plate Model with Bolts

3.2 Objectives of Model Development

The objectives of the computer model development were:

1) To develop a model to generate the information necessary to analyze any base plate configuration,

2) To develop a model which would allow the user to input any size base plate as well as control the size of the elements to be generated for finite element analysis.

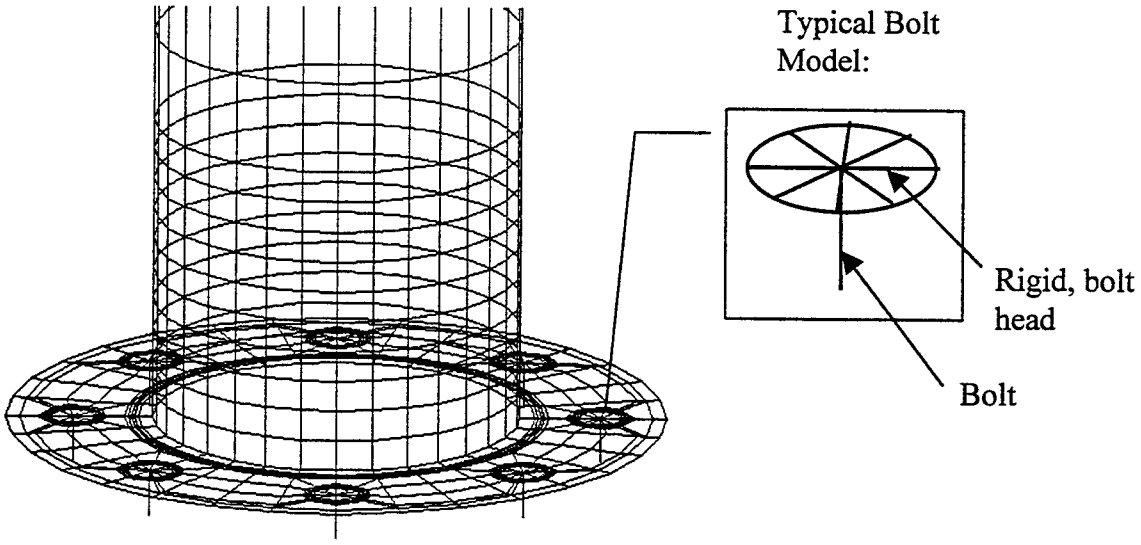

Figure 3.3 Magnified View Showing a Typical Bolt Model

The variables used to generate the base plate model were:

n = Number of bolts

t = Base plate thickness

r_p = Radius of pipe

t_p = Thickness of pipe

r_{bp} = Radius of plate

r_{b1} = Radius of bolts

r_{b2} = Distance from center of pipe to center of bolt

shift_angle = Angle in which the base plate can be shifted for viewing purposes

length = Length of exposed bolt

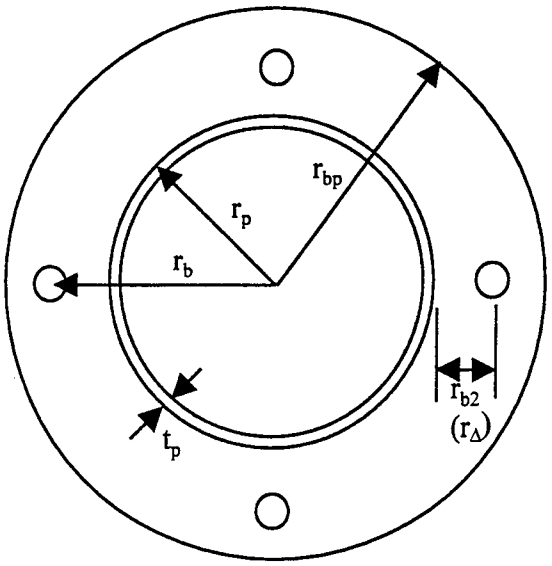

Figure 3.4 Base Plate Variables

The parameters used to generate the elements within the base plate and pipe are:

cb = Number around the bolt

Cbplate = Number around the plate

c = Number of Radial Cuts

c1 = Number of layers in the first section of pipe

c2 = Number of layers in the second section of pipe

c3 = Number of layers in the third section of pipe

t1 = Thickness of layers in the first section of pipe

t2 = Thickness of layers in the second section of pipe

t3 = Thickness of layers in the third section of pipe

The definition of any other input parameters can be found in the SSTAN manual (Hoit, 1995).

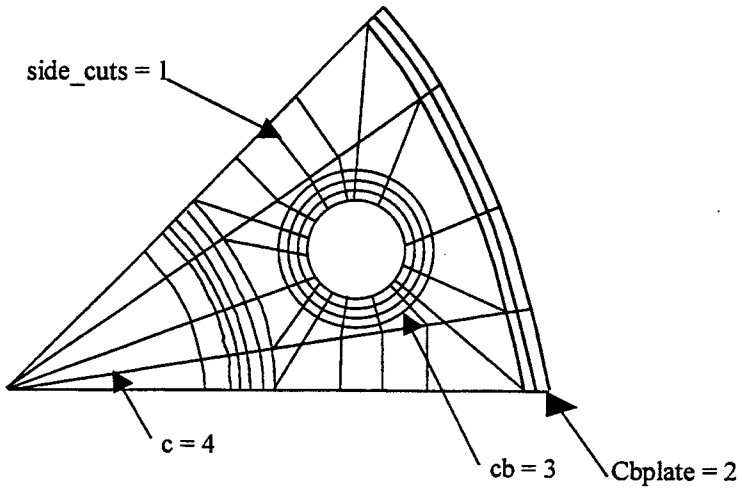

Figure 3.5 Variables for Generation of Elements Within the Base Plate

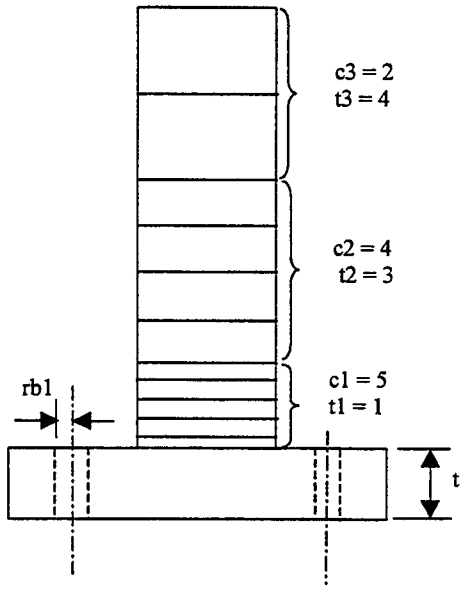

Figure 3.6 Variables for Generation of Elements Within the Pipe

3.3 Development of Subroutines

The computer model serves as a preprocessor to the finite element analysis program, SSTAN (Hoit, 1995). The model is composed of a series of subroutines written in Matlab. The parameters, as mentioned above and in the SSTAN manual, are entered into the file, `batch`. Once the variables are set, typing `plate` at the Matlab command line will run the program. Appendix A provides a line by line listing of the preprocessor.

3.3.1 `Pie`

The subroutine, `pie`, is the first routine the computer runs. This portion of the program generates a pie-like section of the base plate equivalent to $2\pi/(n)$. The x and y coordinates and their corresponding nodes are contained in a matrix, *Node*. Additionally, the elements and their respective node numbers make up the matrix, *Element*.

3.3.2 `Plate`

The routine `plate` duplicates and rotates the nodes and elements created in `pie`, thus producing the entire base plate. This program essentially shifts the coordinates, then generates new nodes that are added to the matrix, *Node*. The same basic procedure is performed on the elements. These nodes and elements are generated through a series of sorting and swapping routines.

3.3.3 `Pipe`

`Pipe` generates the nodes and elements that model the pipe. Three sections of pipe can be created, allowing the most critical sections, closest to the base plate, to contain smaller elements. As shown in Figure 3.6, the number of layers to be contained

in each section and their corresponding thickness are input parameters found in the batch file.

3.3.4 Phase

`Phase` shifts the base plate in its entirety to any angle. The purpose of this routine is to shift the plate in such a way that a bolt is placed on the x-axis for ease of reading the output. The user may use this subroutine to shift the plate any desired angle.

3.3.5 SSTAN

`SSTAN` uses the information generated in the previous routines to create the SSTAN input file. Additional information such as loads, material properties, and beam properties must be entered into the batch file pursuant to the requirements of SSTAN (Hoit, 1995) prior to running the program since, with the possible exception of the proper load placement, this routine completely writes the SSTAN input file. The user must therefore be sure the load is properly applied prior to running this output file through SSTAN (Hoit, 1995).

3.4 Procedure for Usage

This pre-processor allows any base plate configuration and element size to be manually specified. To prevent errors from occurring in the development of the finite element model, the geometry of both the base plate and the elements must be input correctly. The following is a procedure for the usage of the Matlab preprocessor program.

1) At the Matlab command line, type in the correct path for the program (i.e. cd c:\ matlab\phasemdl).
2) Open the file, BATCH, in the folder, phasemdl. See the batch file in Appendix A.
3) The first line, fn='c:\Sstan\filename.inp', is a path used to send the output of the program phasemdl into the SSTAN folder. Replace "filename" with the name of the file to be run. The output will be placed in the SSTAN folder under the given file name.
4) The first twenty parameters (Number_of_bolts through Thickness of base_plate) specify the geometry of the base plate as well as that of the elements to be formed. Input these parameters. It is important to be sure that the geometry of the elements is correct. Check to make sure that there is enough room in between the circle-like elements around the bolt and the elements around the pipe. Also be sure the radial cuts are geometrically allowable around the elements surrounding the bolts. Additionally, the parameter, shift_angle, may be used to place the bolt of the first pie-shaped section on the x-axis. This is done through the equation, 2*pi/(2*Number_of_Bolts). The length_of_exposed_bolt is input as a negative number, representing the portion of the bolt exposed above the concrete.
5) The next thirteen parameters, FX through inc, are used to write the SSTAN input file. Consult the SSTAN manual (Hoit, 1995) for any explanation necessary to complete this section.
6) The final twelve parameters contain the bolt properties. These parameters are also specified in the SSTAN input manual. The bolts are modeled using two material types. The first material is designated for the horizontal beams modeling the top of

the bolt. This portion contains properties that are one hundred times the value of the actual bolt. The second material type is intended for the beam modeling the vertical portion of the bolt. This beam contains the actual properties of the bolt.

a. Consult the AISC Steel Manual (1994) to determine the gross and net areas.

b. Find a weighted area based on the threaded versus unthreaded portions of the bolt. For example,

$$A_{weighted} = A_{net}\left(\frac{L_{threaded}}{L_{total}}\right) + A_{gross}\left(\frac{L_{unthreaded}}{L_{total}}\right) \tag{3-2}$$

Next, find the corrected area for use with the shortened bolt length used in the analysis. This is done to obtain an equivalent axial stiffness for the shortened bolt length, from the surface of the concrete to the base plate, used in the bolt geometry definition. This value is found by dividing the exposed modeled length of the bolt by the length of the bolt from the bottom of the base plate to the uppermost-embedded nut, then multiplying the ratio by the weighted area found in equation (3-2).

$$A_c = A_{weighted}\left(\frac{L_{exposed}}{L_{to\_nut}}\right) \tag{3-3}$$

c. Find the average diameter from the gross and net areas.

d. The moment of inertia can be found by,

$$I = \frac{\pi(d_{average})^4}{64} \tag{3-4}$$

e. The torsional moment of inertia, J, for a circular member, like the bolt, is twice the moment of inertia, I.

7) Once the parameters are set in the batch file, save it.

8) At the Matlab command line, type "plate" and strike the enter key to run the program. It may take several minutes for this program to run. When a new command line prompt appears, the program has finished running.

9) A plan view of the base plate may be seen by typing,"plot(Node(:,2),Node(:,3),'.'" and striking the enter key.

10) If the preprocessing program should stop in the middle, check the geometry and the input, batch file to be sure that everything is correct.

11) Once the preprocessing program is finished, the SSTAN input file can be found in the SSTAN folder under the filename entered in the batch file. This file should have the filename and extension, filename.inp. An example of an input file can be found in Appendix B.

12) Prior to running the file through SSTAN, be sure to check for proper placement of the loads.

13) Run the program through SSTAN. Open the SSTAN program. The program will immediately search for the input file in the SSTAN folder. Highlight the correct file and click the open button on the screen. This program may also take several minutes to process the information. Again, if an error occurs, (i.e. Node numbers not in order) check the geometry of the elements. One method of trouble shooting is to look at the incomplete SSTAN plot to see why the elements are out of order.

14) Once the program has finished analyzing the base plate, open the program SPLOT. Click on FILE, and OPEN. Again, SPLOT will automatically open the SSTAN folder. Find the proper file, highlight it, and click the open button on the screen.

15) Check the SSTAN manual for proper use of the program SPLOT.

16) The output should also be viewed. The output file contains a lot of information about the system analyzed, including the stresses and moments occurring in the elements. This file can be found in the SSTAN folder under "filename.out". Specific sections of the output file can be found in Appendix C.

CHAPTER 4
VERIFICATION OF THE ANALYTICAL MODEL

4.1 Introduction

Once the analytical model was developed, it was important to verify its accuracy. After running the model through SSTAN (Hoit, 1995), several tests were performed to ensure the model was working correctly. The base plates used for this study were the same as those used in the research performed by Cook et al. (1995). The results of the finite element model of the plates were checked against those of the lab tests previously performed to verify accuracy.

4.2 Dimensions of the Base Plate

The dimensions of the base plates used in the previous lab tests are shown below in Table 4.1. The test numbers represent the nominal pipe diameter, the thickness of the base plate, and the number of anchors in the plate. For example, test number 8-3/4-8 refers to a nominal diameter of 203.2 mm (8 in) with a 19.05 mm (¾ in) thick plate and an eight anchor pattern. Likewise, a test numbered 6-1-6 depicts a 152.4 mm (6 in) nominal diameter with a 25.4 mm (1 in) thick plate and a six-anchor pattern. The four-bolt pattern was cast two different ways, in a diamond pattern and in a square pattern. To distinguish between the different tests, the systems using a four-bolt diamond pattern are

designated with "d", such as 6-1-4d. The combination, 6-1-4s uses a square pattern; therefore, it is designated with "s".

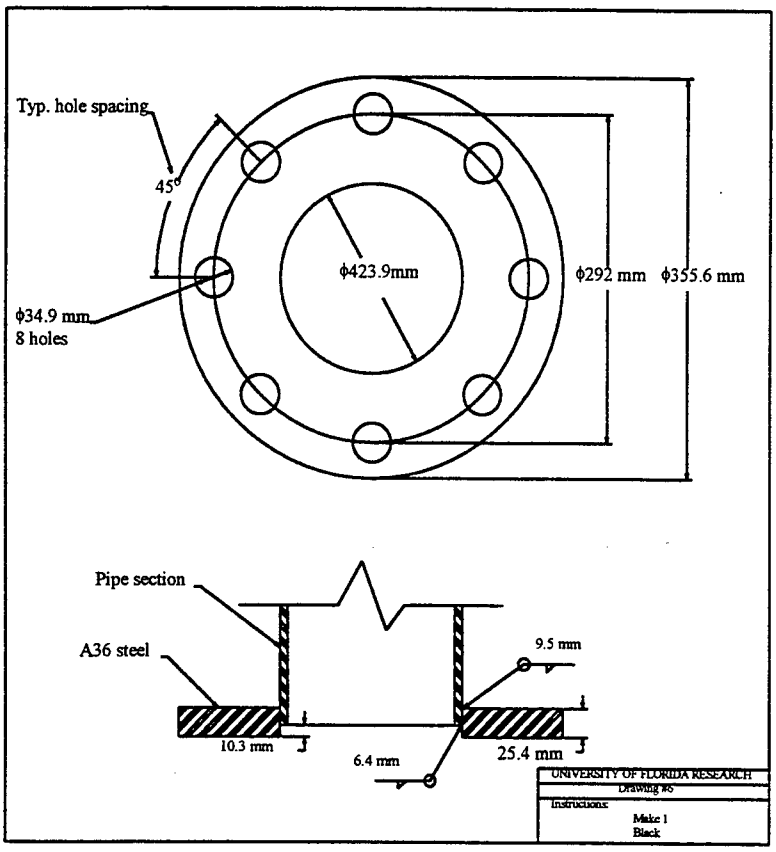

Figure 4.1 Typical Shop Drawing

Table 4.1 Test Dimensions

Test #	Bolt ϕ mm (in)	Pipe ϕ mm (in)	Bolts	Pipe Length mm (in)	Plate Thickness mm (in)
6-1-4d	292 (11.5)	168 (6.63)	4d	1829 (72)	25.4 (1)
6-1-4s	292 (11.5)	168 (6.63)	4s	1829 (72)	25.4 (1)
6/1/06	292 (11.5)	168 (6.63)	6	1829 (72)	25.4 (1)
6/1/08	292 (11.5)	168 (6.63)	8	1829 (72)	25.4 (1)
6-3/4-4d	292 (11.5)	168 (6.63)	4d	1829 (72)	19.1 (3/4)
6-3/4-8	292 (11.5)	168 (6.63)	8	2438 (96)	19.1 (3/4)
8-3/4-4d	292 (11.5)	219 (8.63)	4d	2438 (96)	19.1 (3/4)
8-3/4-6	292 (11.5)	219 (8.63)	6	2438 (96)	19.1 (3/4)
8-3/4-8	292 (11.5)	219 (8.63)	8	2438 (96)	19.1 (3/4)

Additionally, a 25.4 mm (1 inch) anchor bolt was used in all base plate configurations. The length of the bolt from the bottom of the base plate to the top of the uppermost-embedded nut was 495.3 mm.

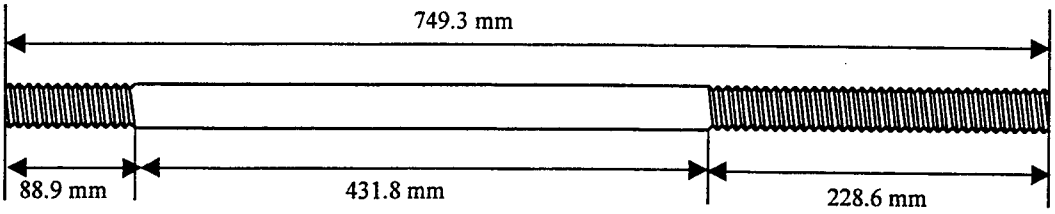

Figure 4.2 Anchor Bolt Detail

4.3 Loads on the System

In the research performed by Cook et al. (1995), it was important to evaluate the deflections occurring in the system in the elastic range since the predictions were made assuming elastic behavior. Although any test value in the elastic range could be compared to the predicted value, it was determined that a comparison of test results at a load level of 50% of the maximum load represented an upper limit to elastic behavior in the tests. These loads were also used in the finite element analyses. Table 4.2 summarizes measured loads and deflections, found in the previous research, at 50% of P_{max}. The deflection shown is measured at the point of application of the load. This point corresponds to the pipe lengths shown in table 4.1

4.4 Deflection from the Pipe

The finite element model was first verified by checking the cantilevered displacement of the pipe. A cantilevered structure, fixed at one end, with a load placed at

Test	50% P_{max} kN (k)	Δ_{total} at 50% P_{max} mm (in)
6-1-4d	16.8 (3.78)	39.6 (1.56)
6-1-4s	20.8 (4.68)	45.5 (1.79)
6-1-6	20.9 (4.70)	41.9 (1.65)
6-1-8	21.8 (4.89)	49.3 (1.94)
6-3/4-4d	10.7 (2.40)	36.8 (1.45)
6-3/4-8	12.8 (2.87)	38.9 (1.53)
8-3/4-4d	12.9 (2.89)	46.2 (1.82)
8-3/4-6	19.9 (4.48)	53.8 (2.12)
8-3/4-8	22.2 (4.98)	63.2 (2.49)

Table 4.2 Summary of Loads and Deflections at 50% P_{max}

the other end produces the deflection below:

$$\Delta_{pipe} = \frac{PL^3}{3EI} + \frac{PL}{AG} \tag{4-1}$$

where,

P = applied load at L

L = length of pipe measured from plate to point of eccentric shear load

E = modulus of elasticity of pipe material

I = moment of inertia of pipe

A = shear area of pipe (Cowper, 1966)

$$A_v = \frac{0.53\pi\left[d_{pipe}^{\ 2} - \left(d_{pipe} - t_{pipe}\right)^2\right]}{4} \tag{4-2}$$

$$G = \frac{E}{2.6} \tag{4-3}$$

G = shear modulus of pipe

Figure 4.3 shows a typical graph of the predicted elastic pipe displacement, Δ_{pipe}, and measured total displacement of a base plate tested in the laboratory (Cook et al., 1995). Notice that the predicted deflection, which consists solely of the deflection of the pipe, is roughly half of that recorded in the lab. This indicates that a large portion of the total deflection is produced by the rotation of the base plate and anchor bolts.

Figure 6-1-6 nent

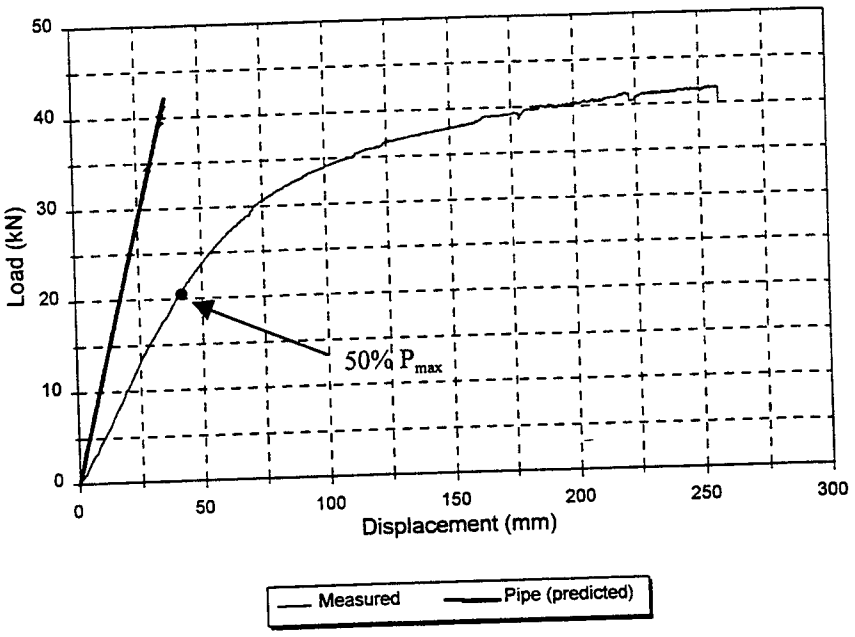

To be sure that the finite element model produced similar results to Equation (4-1), a base plate with a 168 mm pipe was analyzed, fixing all of the nodes at the bottom of the pipe. The deflection from the equation was 3.97 mm (0.1564 in) when a load of 4.448 kN (1 kip) was applied. The resulting deflection from the finite element program was 4.15 mm (0.1635 in), an overestimation of 4.3% of the deflection calculated in Equation (4-1). This was considered to be an acceptable difference for finite element modeling.

4.5 Deflection from the Plate and Bolts

As previously discussed, the bolts were modeled to behave analogously to a spring, using a series of beams. This model resulted in a response equivalent to the flexural and axial deformations, which occurred in the bolts. To model the bolts correctly, the vertical beam modeled the properties of the actual bolt, containing the corrected areas and moment of inertia. The horizontal beams modeled the head of the bolt. These beams were made to be very stiff, containing properties that were 100 times those of the latter beam. The finite element model of the bolts can be seen in Figure 3.3.

A test was first run on this model, making the area of the bolt very large rather than using the corrected area as discussed above. This model allowed flexural bending to occur in the plate, but did not allow any overall plate rotation from axial deformation of the bolts to transpire. The deflection was underestimated by 20% to 50% as seen below in Table 4.3. It was however believed that this model accurately predicted the plate bending.

Table 4.3 Deflection Due to Plate and Pipe Bending

Test #	Deflection (FEM) (mm)	Deflection (Lab) (mm)	FEM/Lab
6-1-4d	27.94	39.62	0.71
6-1-4s	34.95	45.47	0.77
6-1-6	33.40	41.91	0.80
6-1-8	34.09	49.28	0.69
6-3/4-4d	23.34	36.83	0.63
6-3/4-8	25.16	38.86	0.65
8-3/4-4d	22.96	46.23	0.50
8-3/4-6	31.37	53.85	0.58
8-3/4-8	33.05	63.25	0.52

An analysis was then performed on this model using the corrected area of the bolt, as discussed in section 3.4. This test modeled the axial stiffness in the bolts, thus allowing full flexibility to occur within the bolts and the plate. As expected, this analysis increased flexibility, resulting in the greatest overall deflection. The deflections predicted were underestimated by 3% to 30% of the lab data as shown in Table 4.4.

Table 4.4 Deflection Due to Plate, Pipe, and Bolt Bending

Test #	Deflection FEM (mm)	Deflection Lab (mm)	FEM/Lab
6-1-4d	35.56	39.62	0.90
6-1-4s	44.02	45.47	1.00
6-1-6	39.70	41.91	0.90
6-1-8	39.12	49.28	0.79
6-3/4-4d	28.12	36.83	0.76
6-3/4-8	28.30	38.86	0.73
8-3/4-4d	33.02	46.23	0.71
8-3/4-6	42.16	53.85	0.78
8-3/4-8	44.45	63.25	0.70

Spalling occurring around the edges, where the bolt met the concrete edge, was suspected. A model was run using an effective length on the bolt of 3" instead of the 1.5" length used in the prior analysis. There was not a significant change in deflection; however, the difference now ranged from 2% of the actual deflection to 29%. Those values can be seen below in Table 4.5.

Table 4.5 Deflection with an Effective Length of the Bolt of 3"

Test #	Deflection (FEM) (mm)	Deflection (Lab) (mm)	FEM/Lab
6-1-4d	35.94	39.62	0.92
6-1-4s	44.53	45.47	0.98
6-1-6	40.13	41.91	0.96
6-1-8	39.47	49.28	0.80
6-3/4-4d	28.63	36.83	0.78
6-3/4-8	28.88	38.86	0.74
8-3/4-4d	33.83	46.23	0.73
8-3/4-6	43.10	53.85	0.80
8-3/4-8	45.16	63.25	0.71

4.6 Bolt Stiffness

Although the finite element program yielded results that were closer to the deflections found in the lab, the stiffnesses found from LVDT readouts varied from the predicted value. The previous research resulted in bolt stiffnesses ranging from approximately 20000 kN/m to 133333 kN/m. The theoretical stiffness based on the formula, k=AE/L is 157800 kN/m. The observed stiffness ranged approximately from the theoretical value to one-ninth that amount. Since crushing of the concrete can occur

around the embedded portion of the bolt, it was possible to have an observed stiffness that differed from the predicted stiffness. However, it was also possible that the testing equipment used in the previous research was set up incorrectly or there were inconsistencies with the loads on the bolts.

Research performed by Cook and Klinger (1989) indicated the stiffness of the bolt system is approximately one third of the theoretical stiffness. The models of the base plates were run again through the finite element program, using a stiffness of 52600 kN/m. The resulting deflections ranged from an overestimation of 23% to an underestimation of 13%. Those results can be seen below in Table 4.6.

Table 4.6 Application of 1/3 Stiffness

Test #	Deflection (FEM) (mm)	Deflection (Lab) (mm)	FEM/Lab
6-1-4d	48.6664	39.624	1.23
6-1-4s	48.6664	45.466	1.07
6-1-6	51.1048	41.91	1.22
6-1-8	48.1584	49.276	0.98
6-3/4-4d	36.7284	36.83	1.00
6-3/4-8	33.9852	38.862	0.88
8-3/4-4d	51.2064	46.228	1.11
8-3/4-6	61.7474	53.848	1.15
8-3/4-8	59.055	63.246	0.93

Although the resulting deflections were close to the actual deflections, there were still some discrepancies. To rectify this situation, a bolt like the one used in the research

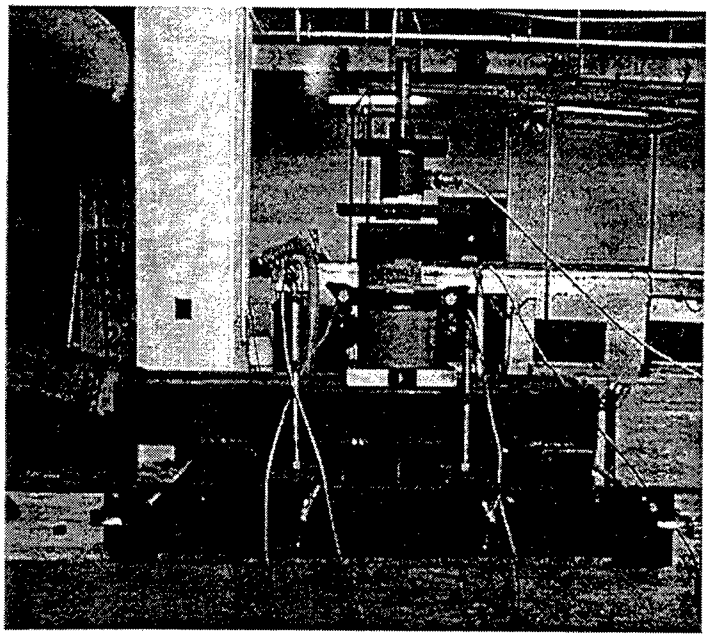

Figure 4.4 Full View: Testing of Bolt Stiffness

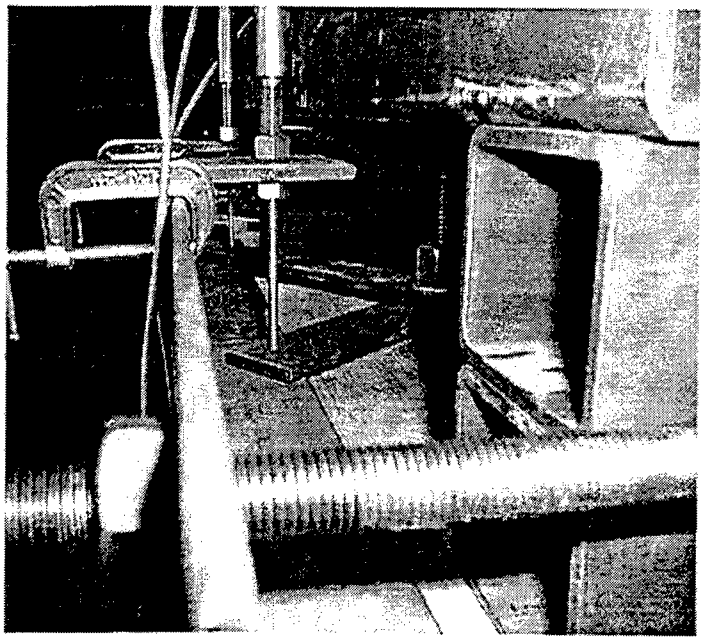

Figure 4.5 LVDT's: Testing of Bolt Stiffness

performed by Cook et al. (1995) was cast in concrete and tested. The test setup is shown in Figures 4.4 and 4.5. The stiffness was found to be approximately 192600 kN/m, which is very close to the predicted value of the stiffness based on the equation, k=AE/L. Therefore, the finite element models that were run using the predicted stiffnesses were determined to be fairly accurate. Since the finite element model underestimated the overall deflection based theoretical stiffness, more testing was recommended.

Since the laboratory tests on the bolts resulted in an average stiffness near the theoretical value, the deflections found in Table 4.4 were determined to be correct. Although the finite element model predicted these deflections within 3% to 30% of those found in the laboratory, the base plates with smaller t_{pipe}/t_{plate} ratios produced better results than the base plates with higher t_{pipe}/t_{plate} ratios.

4.7 Stresses in the Base Plate

It was also important to check the stresses that were occurring in the base plate to determine whether the system was in the elastic or inelastic range. Coupon tests performed during the previous research (Cook et al., 1995) resulted in strengths as shown below in Table 4.7.

Since there were several hundred nodes in the model, it would not be feasible to check every node. Therefore, the most critical node of the system was checked. Since shell elements were used to model the system it was necessary to calculate the stress using Equations (4-4) and (4-5).

Table 4.7 Tensile Test Results for the Base Plate

Plate Thickness mm (in.)	Coupon #	F_y MPa (ksi)	Average F_y MPa (ksi)	F_u MPa (ksi)	Average F_u MPa (ksi)
25.4 (1)	1	372 (54.0)	362 (52.5)	675 (97.8)	669 (97.0)
	2	352 (51.0)		664 (96.2)	
19.1 (3/4)	1	346 (50.2)	382 (55.4)	543 (78.7)	581 (84.2)
	2	417 (60.5)		619 (89.8)	

$$\sigma_x = \sigma_{My} + \sigma_{Nx} \tag{4-4}$$

$$\sigma_x = \frac{6M_y}{t_{plate}^2} + \sigma_{Nx} \tag{4-5}$$

where,

σ_x = stress of the elements

σ_{Nx} = Stress in the x direction, found in the SSTAN output file

M_y =Moment about the y-direction, found in the SSTAN output file

t_{plate} = Thickness of the base plate

As shown below in Table 4.8, the stresses do not exceed the yielding point. Therefore, an elastic analysis is sufficient.

Additionally, the stresses in the pipe were checked. The pipes used in the preceding research (Cook et al., 1995) were ASTM A53 Type E, Grade B, Standard Weight. For an A53 pipe, the minimum yield strength is 248 MPa; however, yielding typically occurs at 345 MPa.

Table 4.8 Stresses in the Base Plate at the Most Critical Point

Test #	σ_{Nx}(ave) MPa	My(ave) kN-m	σ_{My} MPa	σ_x(total) MPa
6-1-4d	16.25	0.26	94.41	110.65
6-1-4s	16.50	0.39	144.38	160.88
6-1-6	19.59	0.35	129.43	149.01
6-1-8	20.80	0.34	126.12	146.91
6-3/4-4d	18.92	0.27	177.65	196.58
6-3/4-8	21.85	0.32	208.91	230.76
8-3/4-4d	18.69	0.25	162.69	181.37
8-3/4-6	26.24	0.41	268.26	294.50
8-3/4-8	28.10	0.40	262.41	290.51

The output file of the program, SSTAN, presented the stresses in a local coordinate system. The stresses were therefore calculated using Equation (4-4). Most of the stresses were below 245 MPa. Although test 6-1-8 had a stress of 274 MPa, which is above the minimum yielding point for the pipes analyzed, it probably did not yield since the yielding point was most likely around 345 MPa. Therefore, the pipe remained in the elastic range as shown below in Table 4.9.

Table 4.9 Stresses in Pipes

Test #	σ_{Nx}(ave) MPa	My(ave) kN-m	σ_{My} MPa	σ_x(total) MPa
6-1-4d	69.98	0.006	2.20	72.18
6-1-4s	223.33	0.06	21.95	245.28
6-1-6	219.47	0.06	21.95	241.42
6-1-8	248.50	0.07	25.61	274.11
6-3/4-4d	102.32	0.04	26.02	128.34
6-3/4-8	145.21	0.06	39.02	184.23
8-3/4-4d	98.39	0.06	39.02	137.41
8-3/4-6	145.42	0.1	65.04	210.46
8-3/4-8	168.93	0.1	65.04	233.97

CHAPTER 5
DEVELOPMENT OF DESIGN MODEL

As previously discussed, most engineers calculate the deflection of lighting poles and mast arms as cantilevered beams, fixed at one end. This approach assumes that the deflection comes entirely from the pipe. As discovered in this and previous research (Cook et al., 1995), deflection does not come from the pipe alone. Three factors were found to contribute to the overall deflection of the annular base plate structure. Those factors are given in Equation (5-1):

$$\Delta = \Delta_{pipe} + \Delta_{bolt} + \Delta_{plate} \tag{5-1}$$

Figure 5.1 better illustrates the source of the deflections mentioned above.

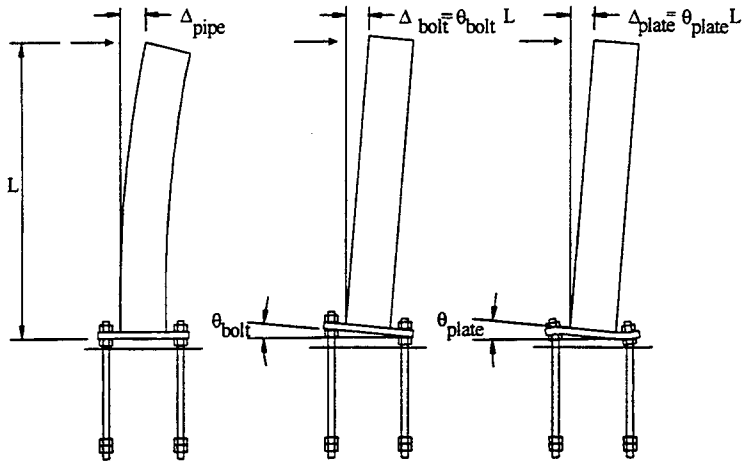

Figure 5.1 Components of Total Deflection

5.1 Parameters of the Base Plates

A parameter study was performed on several base plate systems. Specific parameters were varied, evaluating the manner in which the rotation changes. The base plates studied had the geometric make-up of the smallest base plate, the largest base plate, and an additional base plate typically used by the FDOT. The test designations below are the same as those of the previous research. For example, test 10-1-6 has a ten-inch diameter pipe with a 1" thick plate and 6 bolts. The basic geometries of these base plates are shown below in Table 5.1.

Table 5.1 Base Plate Geometries

Property:		10-1-6	25-2.375-8	24-2-12
		mm (in)	mm (in)	mm (in)
Number of Bolts	N	6	8	12
Radius of Pipe	r_p	127 (5)	317.5 (12.5)	304.8 (12)
Radius to Bolt Center	r_b	157.75 (6.25)	419.1 (16.5)	393.7 (15.5)
Outer Diameter	OD	381 (15)	1041.4 (41)	939.8 (37)
Plate Thickness	t	25.4 (1)	60.325 (2.375)	50.8 (2)
Pipe Thickness	t_p	4.935 (0.1943)	9.525 (0.375)	9.525 (0.375)
Diameter of Bolt	d_b	15.875 (5/8)	50.8 (2)	38.1 (1.5)

5.2 Rotation from the Plate

The base plate configurations discussed in section 5.1 were analyzed using the finite element program, SSTAN (Hoit, 1995). Parameters, such as the plate thickness or the diameter of the bolt were varied to evaluate the effect on the plate rotation.

In order to evaluate plate rotation by itself, the axial stiffness of the bolts was artificially increased, thus eliminating the portion of the total rotation coming from axial deformation in the bolts. Flexural bending of the bolts was included since it directly effected plate rotation. The rotation of the plate was then found using equation (3-1).

Similar base plate configurations were used in the analyses, varying specific parameters. For the first analysis, the thickness of the base plate was the only parameter varied. In the second analysis, two parameters were varied, the bolt diameter, d_b, and the distance from the pipe's edge to the center of the bolt, r_Δ, where $r_\Delta = r_b - r_p$. According to FDOT specifications, the distance from the edge of the pipe to the center of the bolt, and the distance from the center of the bolt to the outer edge of the base plate are both equal to twice the bolt diameter. Therefore, by changing the diameter of the bolt, the parameter, r_Δ changes. The results of the analyses were plotted against the ratio, r_Δ / t_{plate}. It was found that for $r_\Delta / t_{plate} \geq 1$, the relationship between the rotation of the base plate and r_Δ / t_{plate} was nearly linear.

5.2.1 Development of Equation for Plate Bending

An equation for plate rotation was derived, treating the plate as a beam supported at the bolts. Both the rotations due to flexure and shear were included in the derivation. Figure 5.2 shows the basic model used to develop the design equation. The equation for plate rotation is shown below in Equation (5-2).

$$\theta_{plate} = \theta_{flexure} + \theta_{shear} \tag{5-2}$$

Beam Model:

Flexural Rotation:

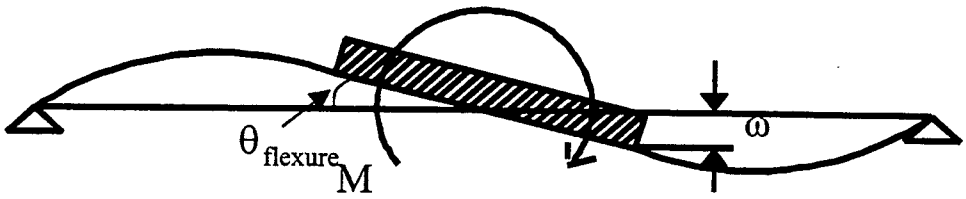

Shear Rotation:

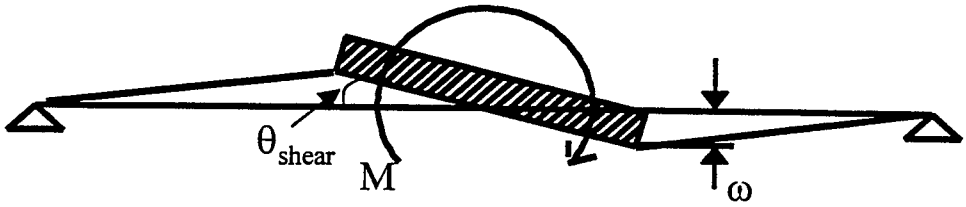

Figure 5.2 Beam Model Used for the Design Equation

The moment of inertia was estimated based on the changing geometry of the plate. The moment of inertia was estimated in Equation (5-3):

$$I_x = I_o \frac{x}{r_\Delta} \tag{5-3}$$

where,

$$I_o = \frac{b t_{plate}^{\ 3}}{12}$$

$$b = 2\sqrt{r_b^{\ 2} - r_p^{\ 2}}$$

Below, Figure 5.3 shows how the width, b varies along the base plate.

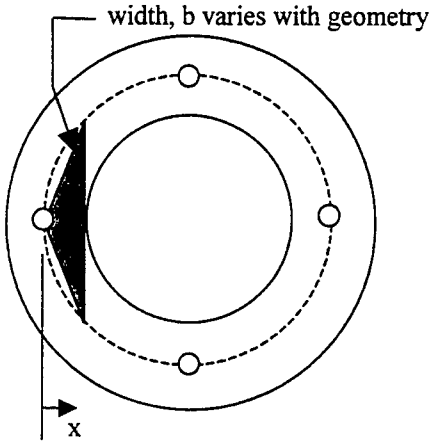

Figure 5.3 Calculation of Moment of Inertia

The calculation of the rotation of the plate due to shear is given in Equation (5-4):

$$\theta_{shear} = \frac{M}{2AG}\frac{r_\Delta}{r_b^{\,2}} \tag{5-4}$$

where,

M = moment applied to system

$$A = 2\sqrt{r_b^{\,2} - r_p^{\,2}}\, t_{plate}$$

$$G = \frac{E}{2.6}$$

$$r_\Delta = r_b - r_p$$

As previously stated, there was a linear relationship between r_Δ/t_{plate} and the rotation due to the plate bending. To better understand the system, the equation for shear was written in terms of r_Δ/t_{plate} in equation (5-5).

$$\theta_{shear} = \frac{1.3M}{Er_b^{\,2}b}\frac{r_\Delta}{t_{plate}} \tag{5-5}$$

The rotation of the plate was also due to flexure. The derivation is presented in Equation (5-6):

$$\theta_{flexure} = \frac{M}{4EI_o}\frac{r_\Delta^3}{r_b^2} \tag{5-6}$$

The rotation from flexure can also be written in terms of r_Δ/t. However that term is in a cubic form.

$$\theta_{flexure} = \frac{3M}{Er_b^2 b}\left(\frac{r_\Delta}{t_{plate}}\right)^3 \tag{5-7}$$

The equation developed for plate rotation was found by combining Equations (5-5) and (5-7):

$$\theta_{plate} = \frac{3M}{Er_b^2 b}\left(\frac{r_\Delta}{t_{plate}}\right)^3 + \frac{1.3M}{Er_b^2 b}\frac{r_\Delta}{t_{plate}} \tag{5-8}$$

As shown in the formulas above, in a system where flexure governed the rotation, the rotation plotted against r_Δ/t_{plate} would produce a cubic response. From the deflected picture in Figure 5.4, it is evident that the finite element model produced a linear response, much like one that would be produced by the shear equation.

Figure 5.4 shows the deflected picture of a typical FDOT base plate. The pipe thickness is relatively small in comparison to the thickness of the plate. Due to the small pipe to plate ratio, there is not enough flexural rigidity to prevent rotation of the pipe, thus resulting in a hinge-like action at the pipe and plate interface. Additionally, a

bending reaction occurs in the pipe toward the bottom as demonstrated in the blown up portion of Figure 5.4.

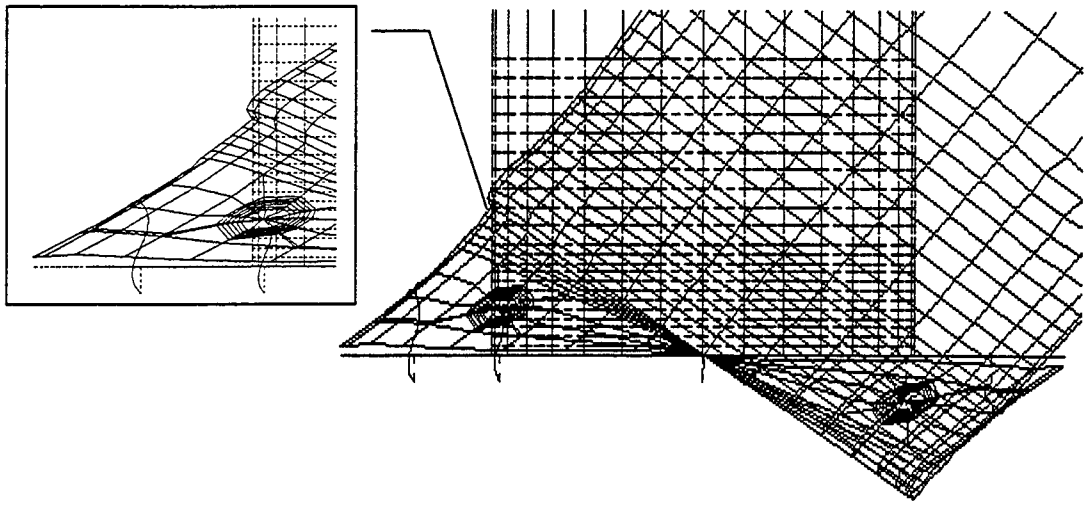

Figure 5.4 Hinge-Like Effect of a Typical Base Plate

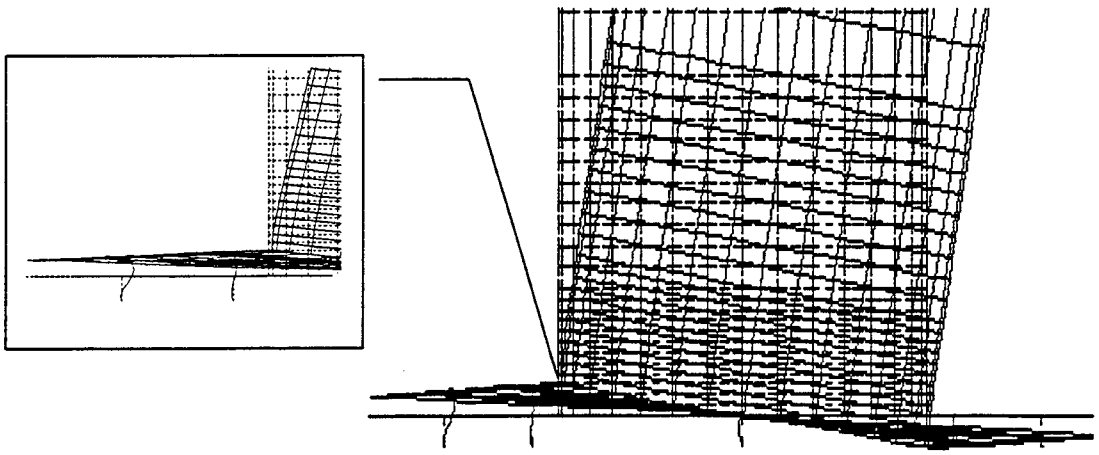

Figure 5.5 No Hinge-Like Response when Pipe Thickness Equals Plate Thickness

The plate thickness was then set equal to the pipe thickness. This time, the thick pipe had enough flexural rigidity to prevent the rotation. That rigidity also prevented the bulging effect from occurring in the pipe. A deflected picture of the pipe thickness equaling the plate thickness is shown in Figure 5.5. Note that Figures 5.4 and 5.5 were produced using the same applied load.

According to Young (1989), there is an additional deflection due to shear in every case of plate bending. In many cases, this deflection was so slight, that it was negligible; however, Young says that in circular plates with large openings, the deflection due to shear may constitute a considerable portion of the total deflection. Wahl and Lobo (1933) states that this should occur when the thickness is greater than one-third the difference between the inner and outer diameters, r_Δ, for plates with simply supported edges. This was the case for all of the base plates analyzed, as well as all typical FDOT base plate systems. Figure 5.6 shows typical relationships between r_Δ and t_{plate}.

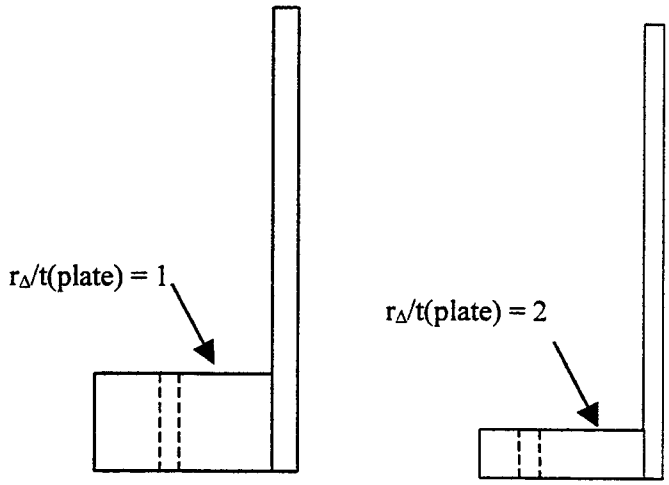

Figure 5.6 Typical FDOT Base Plate Systems

Since shear constituted a considerable portion of the rotation occurring in FDOT base plates, it was necessary to calibrate the equation for plate rotation to mirror that effect. Although a considerable portion of the rotation was from shear, there was still some flexure occurring in the system; therefore, it was necessary to incorporate that portion of the equation into the calculation of the overall rotation.

To determine the calibration factor, the actual rotation due to shear, resulting from the finite element analysis was compared to the calculated rotation due to shear, found in Equation (5-5). In order to obtain the finite element model (FEM) rotation due solely to shear, the pipe deflection and rotation due to plate flexure was removed. A calibration factor was then calculated by dividing the FEM rotation from shear by the calculated rotation from shear. An average difference was taken from all of the models analyzed. The calibration factor was found to be 42. This factor was used to magnify the considerable shear-like effect shown above in Figure 5.4. The full equation for plate bending is demonstrated below in Equation (5-9):

$$\theta_{plate} = \frac{M}{4EI_{plate}} \frac{r_{\Delta}^{3}}{r_{b}^{2}} + \frac{21M}{AG} \frac{r_{\Delta}}{r_{b}^{2}} \tag{5-9}$$

where,

$I_{plate} = bt_{plate}^{3}/12$

$A = bt_{plate}$

$G = E/2.6$

$$b = 2\sqrt{r_b^{\,2} - r_p^{\,2}}$$

The equation for plate rotation can be written in terms of the ratio r_Δ/t_{plate}:

$$\theta_{plate} = \frac{3M}{Er_b^{\,2}}\left(\frac{r_\Delta}{t_{plate}}\right)^3 + \frac{55M}{Er_b^{\,2}b}\left(\frac{r_\Delta}{t_{plate}}\right) \qquad (5\text{-}10)$$

Since Equation (5-9) was not dependent on the number of bolts, it was important to be sure that the rotation from the base plate system did not change with the changing bolt number. Two base plates were analyzed, changing the bolt condition. A base plate similar to the ones used in the laboratory (Cook et al., 1995) was evaluated in addition to base plate 25-2.375-8. There was no significant change in the rotation based on the number of bolts used in a base plate. The lab base plate was evaluated using 4, 6, and 8 bolts. The calculated rotations were found to be within 3% of the average. Similarly, plate 25-2.375-8 was analyzed using 6, 8, and 10 bolts. The calculated rotations were predicted within 4% of the average value.

5.2.2 Verification of Equation for Plate Rotation Using Typical FDOT Base Plates

Equation (5-9) was analyzed varying the critical parameters, as discussed at the beginning of section 5.2. The equation was found to estimate the plate rotation well within reasonable ranges. Those ranges were specified based on typical FDOT installations, and are shown below in Table 5.2. The FEM and calculated rotations were graphed against the ratios, r_Δ/t_{plate} and t_{plate}/d_{bolt}. The results can be seen below in Tables 5.3 and 5.4. Table 5.4 shows the results of varying r_Δ by varying the bolt diameter according to FDOT specifications. As previously stated those specifications state that the

distance, r_{Δ}, should be equal to twice the bolt diameter. The test names represent the number of bolts, the diameter of the bolts, the plate diameter, and the thickness. For example, plate 6-0625-15-100 represents a six-bolt configuration with a 15.875 mm (0.625 in) bolt diameter, a 381 mm (15 in) plate diameter, and 25.4 mm (1 in) plate thickness.

Table 5.2 Ranges of Typical FDOT Base Plate Systems

Limits:	F.D.O.T. Ranges
r(Δ)/t(plate)	1 to 2
t(pipe)/t(plate)	< 0.4
t(plate)/d(bolt)	1 to 2
t(plate)	≥ 0.75

Table 5.3 Results of Varying Plate Thickness

Base Plate: 10-1-6			
Thickness	θ_{plate} (FEM)	θ_{plate} (calculated)	Calculated/FEM
19.05	1.11E-03	8.89E-04	0.80
25.40	6.48E-04	6.28E-04	0.97
31.75	4.26E-04	4.88E-04	1.14
Base Plate: 25-2.375-8			
Thickness	θ_{plate} (FEM)	θ_{plate} (calculated)	Calculated/FEM
50.80	6.36E-05	5.64E-05	0.89
57.15	5.11E-05	4.82E-05	0.94
60.33	4.59E-05	4.50E-05	0.98
63.50	4.13E-05	4.22E-05	1.02
69.85	3.37E-05	3.75E-05	1.11
76.20	2.76E-05	3.38E-05	1.21
Base Plate: 24-2-12			
Thickness	θ_{plate} (FEM)	θ_{plate} (calculated)	Calculated/FEM
44.45	8.31E-05	7.02E-05	0.85
50.80	6.50E-05	5.88E-05	0.90
57.15	5.10E-05	5.07E-05	0.99
63.50	4.02E-05	4.46E-05	1.11
69.85	3.19E-05	3.99E-05	1.25

Table 5.4 Results of Varying r_Δ by Varying d_{bolt}.

Plate	θ_{plate} (FEM)	θ_{plate} (calculated)	Calculated/FEM
6-0625-15-100	6.22E-04	6.28E-04	1.01
6-075-16-100	6.99E-04	6.51E-04	0.94
6-0875-17-100	7.59E-04	6.71E-04	0.89
6-100-18-100	8.24E-04	6.89E-04	0.83
8-125-35-200	5.28E-05	4.93E-05	0.94
8-150-37-200	5.79E-05	5.19E-05	0.89
8-175-39-200	6.10E-05	5.42E-05	0.89
8-200-41-200	6.36E-05	5.64E-05	0.89

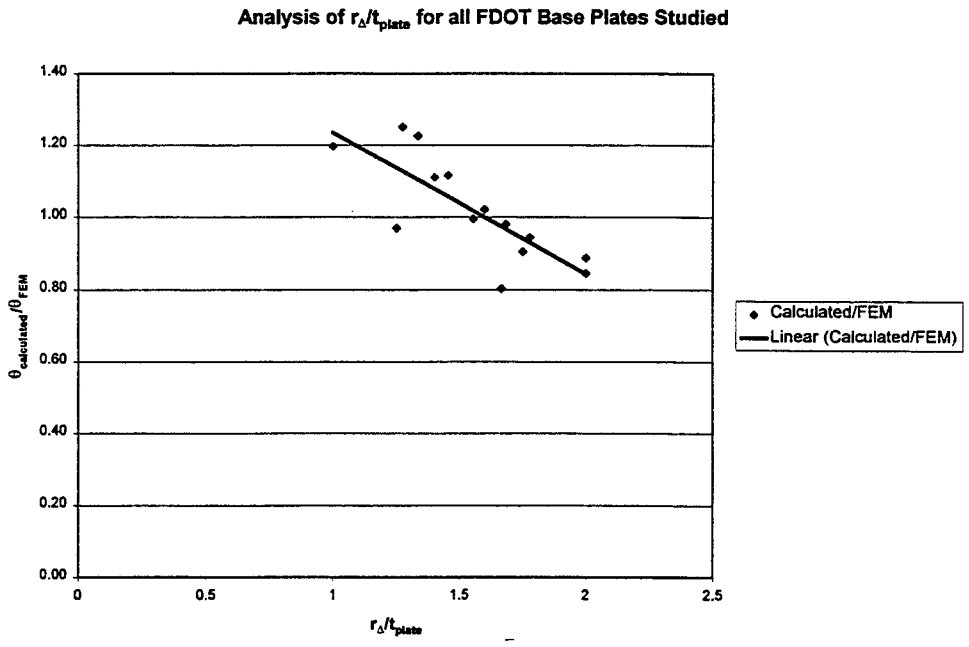

Figure 5.7 Graph of r_Δ/t_{plate} vs. $\theta_{calculated}/\theta_{FEM}$ for FDOT Base Plates Analyzed Over Varying Thickness

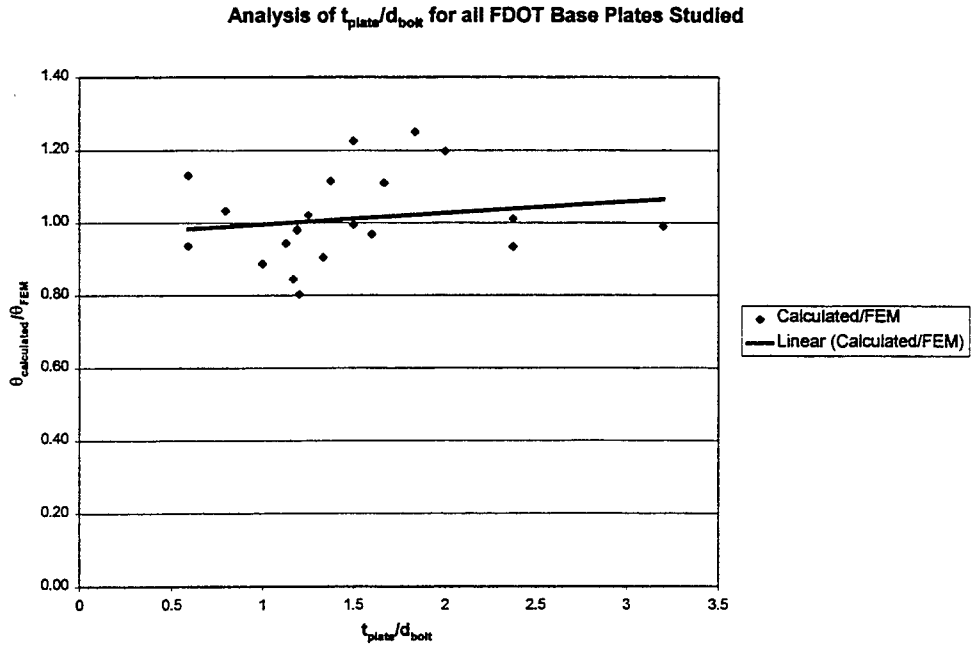

Figure 5.8 Graph of t_{plate}/d_b vs. $\theta_{calculated}/\theta_{FEM}$ for FDOT Base Plates Analyzed Over Varying Thickness

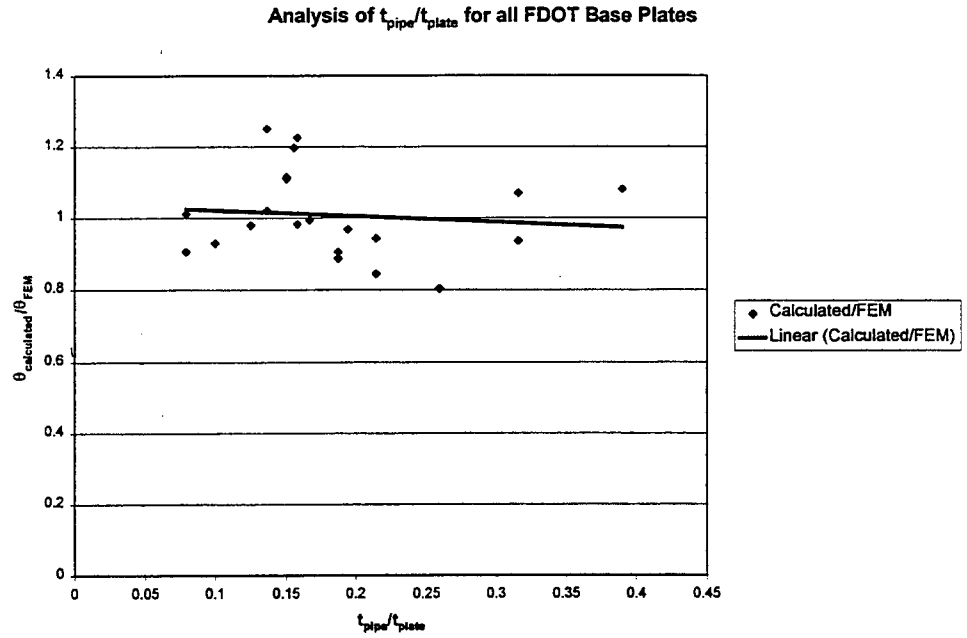

Figure 5.9 Graph of t_{pipe}/t_{plate} vs. $\theta_{calculated}/\theta_{FEM}$ for FDOT Base Plates Analyzed Over Varying Thickness

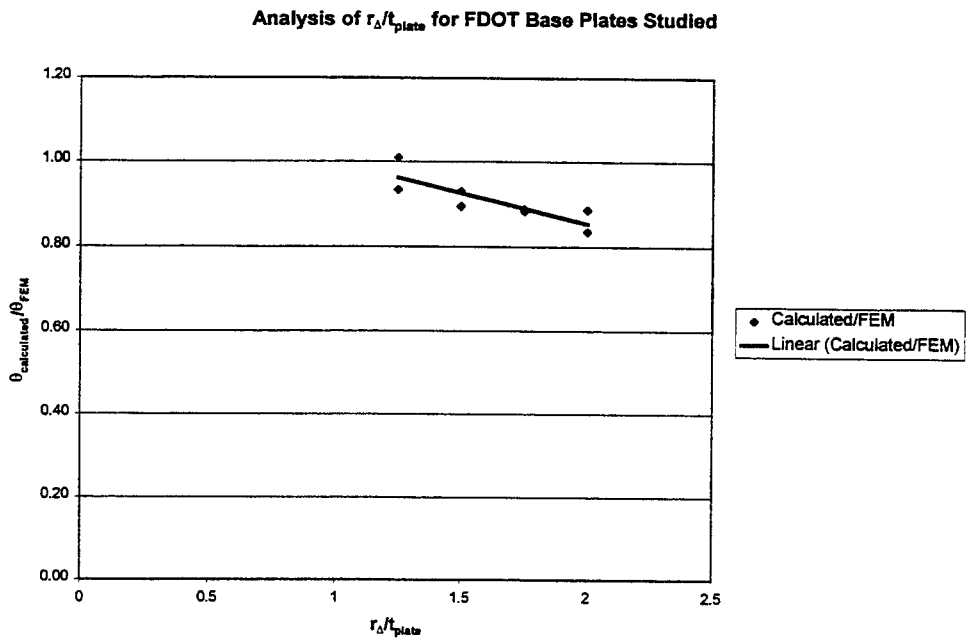

Figure 5.10 Graph of r_Δ/t_{plate} vs. $\theta_{calculated}/\theta_{FEM}$ for FDOT Base Plates Analyzed Over Varying r_Δ and d_b

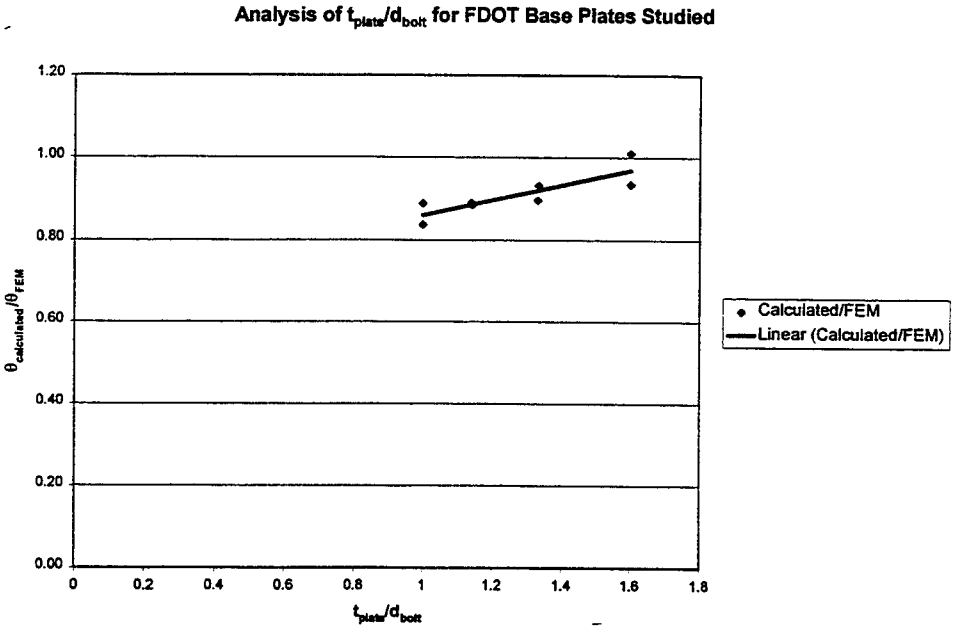

Figure 5.11 Graph of t/d_b vs. $\theta_{calculated}/\theta_{FEM}$ for FDOT Base Plates Analyzed Over Varying r_Δ and d_b

5.2.3 Analysis of Equation for Plate Rotation Using Extreme Parameter Values

Additionally, a study was performed varying critical parameters to extreme values. The smallest and the largest base plates typically used by FDOT were used in this analysis. The basic parameters of these base plates are shown below, in Tables 5.5 and 5.8, and above, in Table 5.1. The parameters varied in this analysis were the plate thickness (t_{plate}), the distance from the edge of the pipe to the center of the bolt (r_{Δ}), the pipe thickness (t_{pipe}), and the bolt diameter (d_{bolt}). These variables were individually divided in half, then evaluated with a finite element analysis and compared to Equation (5-9); and likewise, multiplied by two, then evaluated. The results can be found below in Tables 5.5 through 5.10.

Table 5.5 Varying Critical Parameters to Extreme Values: Small Base Plate

Small Base Plate:						
	θ_{plate} (FEM)	θ_{plate} (FEM)	θ_{plate} (FEM)	θ_{plate} (calculated)	θ_{plate} (calculated)	θ_{plate} (calculated)
Variable (V):	0.5 X V	1 X V	2 X V	0.5 X V	1 X V	2 X V
t(plate) = 25.4 mm	1.92E-03	6.48E-04	1.84E-04	1.55E-03	6.28E-04	2.95E-04
r(Δ) = 31.75 mm	5.03E-04	6.48E-04	9.26E-04	4.07E-04	6.28E-04	7.24E-04
t(pipe) = 4.94 mm	5.82E-04	6.48E-04	6.79E-04	6.28E-04	6.28E-04	6.28E-04
d(bolt) = 15.89mm	6.34E-04	6.48E-04	6.08E-04	6.28E-04	6.28E-04	6.28E-04

Table 5.6 Ratio of the FEM and Calculated Values: Small Base Plate

	Calc/FEM	Calc/FEM	Calc/FEM
Ratio:	0.5 X V	1 X V	2 X V
t(plate) = 25.4 mm	0.81	0.97	1.60
r(Δ) = 31.75 mm	0.81	0.97	0.78
t(pipe) = 4.94 mm	0.93	0.97	1.08
d(bolt) = 15.89 mm	0.99	0.97	1.03

Table 5.7 Values of Critical Ratios for the Small Base Plate

		t_{plate}:			r_{Δ}:			t_{pipe}:			d_{bolt}:		
Ratios:	FDOT Ranges	0.5V	1V	2V	0.5V	1V	2V	0.5V	1V	2V	0.5V	1V	2V
r_{Δ}/t_{plate}	1 to 2	2.50	1.25	0.625	0.625	1.25	2.50	--	--	--	--	--	--
t_{plate}/d_{bolt}	1 to 2	0.80	1.60	3.20	--	--	--	--	--	--	3.20	1.60	0.80
t_{pipe}/t_{plate}	> 0.4	0.39	0.19	0.10	--	--	--	0.10	0.19	0.39	--	--	--
t_{plate}	≥19mm	12.7	25.4	50.8	--	--	--	--	--	--	--	--	--

Table 5.7 depicts the values of the ratios found critical in this study. This table also shows how the extreme parameter values compare to the typical ranges for the small base plate.

Although Equation (5-9) was able to predict the plate rotation within reasonable limits for most of the tests, the rotation was not accurately predicted when plate thickness was doubled. It was important to take note that many of the parameters evaluated at their extremes, either at one half the typical value or twice that value, were within FDOT ranges specified in Table 5.2. The thickness of 50.8 mm, which possessed an r_{Δ}/t_{plate} value of 0.53 was over-predicted by a factor of 1.5. Additionally, the ratio of plate thickness to bolt diameter was 3.25. The range for the ratio of t_{plate}/d_{bolt} should not go beyond a value of two.

The large base plate was also evaluated using the same extreme criteria. As shown below, most of the parameters analyzed were predicted within reasonable limits. The results of that analysis can be seen below in Tables 5.8 through 5.10.

Table 5.8 Varying Critical Parameters to Extreme Values: Large Base Plate

Large Base Plate:						
	θ_{plate} (actual)	θ_{plate} (actual)	θ_{plate} (actual)	θ_{plate} (predicted)	θ_{plate} (predicted)	θ_{plate} (predicted)
Variable (V):	0.5 X V	1 X V	2 X V	0.5 X V	1 X V	2 X V
t(plate) = 60.325 mm	1.35E-04	4.58E-05	2.00E-05	1.26E-04	4.50E-05	2.02E-05
r(Δ) = 101.6 mm	1.37E-05	4.58E-05	7.85E-05	2.77E-05	4.50E-05	4.96E-05
t(pipe) = 9.525 mm	4.97E-05	4.58E-05	4.21E-05	4.50E-05	4.50E-05	4.50E-05
d(bolt) = 50.8 mm	4.82E-05	4.58E-05	3.98E-05	4.50E-05	4.50E-05	4.50E-05

Table 5.9 Difference Between the Actual and Predicted Values: Large Base Plate

	Calc/FEM	Calc/FEM	Calc/FEM
Ratio:	0.5 X V	1 X V	2 X V
t(plate) = 60.325 mm	0.94	0.98	1.01
r(Δ) = 101.6 mm	2.00	0.98	0.63
t(pipe) = 9.525 mm	0.91	0.98	1.06
d(bolt) = 50.8 mm	0.94	0.98	1.14

Table 5.10 Values of Critical Ratios for the Large Base Plate

		t_{plate}:			r_{Δ}:			t_{pipe}:			d_{bolt}:		
Ratios:	FDOT Ranges	0.5V	1V	2V	0.5V	1V	2V	0.5V	1V	2V	0.5V	1V	2V
r_{Δ}/t_{plate}	1 to 2	3.37	1.68	0.84	0.84	1.68	3.37	--	--	--	--	--	--
t_{plate}/d_{bolt}	1 to 2	0.59	1.19	2.38	--	--	--	--	--	--	2.38	1.19	0.59
t_{pipe}/t_{plate}	> 0.4	0.32	0.16	0.08	--	--	--	0.08	0.16	0.32	--	--	--
t_{plate}	≥19mm	30.2	60.3	120.7	--	--	--	--	--	--	--	--	--

Again the analysis on the large base plate was performed at extreme values. Many of these studies, like those of the small base plate, did not fall within the FDOT ranges specified in Table 5.2. The only problems found were in the analysis of varying

the value, r_Δ. The large base plate, at the lower extreme, had an r_Δ value of 50.8 mm, corresponding to an r_Δ/t_{plate} ratio equal to 0.84. The rotation of the large base plate was overpredicted by a factor of 2. Additionally, when r_Δ was set to 203.2 mm, twice the typical value, the rotation was under predicted by a factor of 1.58. The ratio of r_Δ/t_{plate} was calculated as 3.37.

To be sure equation (5-9) was accurately predicting rotations, the upper and lower limits of r_Δ were analyzed. Firstly, r_Δ was set to 50.38 mm. The ratio, r_Δ/t_{plate} was calculated to be one. The actual rotation was 3.21×10^{-5} and the predicted rotation was 4×10^{-5}. The plate rotation was predicted over the actual value by a factor of 0.80. Secondly, r_Δ was changed to 120.55 mm, which corresponded to an r_Δ/t_{plate} ratio of two. The actual rotation was found to be 5.58×10^{-5}. The rotation was predicted with a factor of 1.2 to be 4.58×10^{-5}. Since both ends of the range for the large base plate were found to calculate the plate rotation within reasonable limits, the equation was still found to be adequate.

5.3 Development of Equation for Bolt Rotation

Finally, a portion of the unaccounted deflection came from the anchor bolts. When the system was loaded, the compression bolts shortened while the tension bolts elongated. A rigid body rotation of the base plate occurred as a result of this event as shown in Figure 5.12.

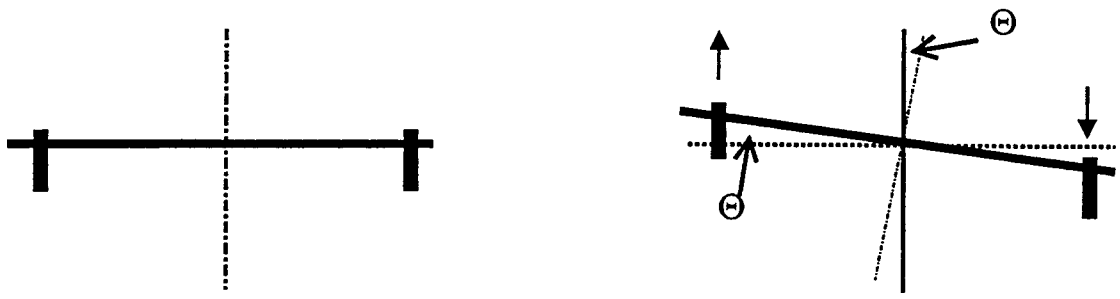

Figure 5.12 Rotation of System Due to Bolts

The equation for bolt rotation was based on the theoretical equation for axial deflection of the outermost anchor in a group of anchor bolts in the elastic range:

$$\Delta_{bolt} = \frac{ML_b}{s_g A_b E_b} \tag{5-11}$$

where,

M = applied moment on anchor group

L_b = length of bolt under tension or compression (521 mm for all tests)

s_g = unit section modulus of bolt group relative to the axis of moment application

$$s_g = \frac{\sum \bar{y}_b^2}{y_{max}} \tag{5-12}$$

y_b = distance from the centroid of the bolt group to a particular bolt

y_{max} = distance from the centroid of the bolt group to the outermost bolt

A_b = cross-sectional area of the bolt

E_b = modulus of elasticity of the bolt

The overall rotation due to the bolts was calculated by dividing equation (5-11) by the distance from the center of the plate to the center of the bolts.

$$\theta_{bolt} = \frac{ML_b}{s_g A_b E_b r_b} \tag{5-13}$$

r_b = distance from the center of the plate to the center of the outermost bolt

To determine the actual rotation due to the bolts, two analyses were performed using the finite element program. The first test, as previously discussed, was run, making the axial stiffness of the bolts very large. This study allowed the plate bending to occur, but prevented the bolt rotation to transpire. The second analysis was performed, using the actual bolt stiffness, which allowed the bolt rotation to occur as well as the rotation due to the plate. Finally, the analysis in which the plate rotation solely occurred was subtracted from that of full rotation of the system. The resulting rotation came from the bolts.

Cook et al. (1995) found that a factor of 1.5 should be applied to equation (5-13) to properly account for the bolts. An analysis was performed using the finite element analysis program to see if the base plates evaluated in this study also required a factor of 1.5. The results are shown below in Table 5.11. Equation (5-13) was used to calculate the rotations in Table 5.11.

The average difference was calculated to be 1.45 with a coefficient of variation of 10%. A factor of 1.5, applied to equation (5-13), was found to be reasonable, as shown in Equation (5-14).

$$\theta_{bolt} = \frac{1.5ML_b}{s_g A_b E_b r_b} \tag{5-14}$$

Table 5.11 Comparison of Calculated and Actual Bolt Rotations

Test 10-1-6:			
Thickness	θ_{bolts} (FEM)	θ_{bolts} (calculated)	(FEM/Calculated) (No Factor Applied)
0.75	1.64E-03	1.23E-03	1.34
1	1.62E-03	1.23E-03	1.32
1.25	1.61E-03	1.23E-03	1.32
Test 25-2.375-8:			
Thickness	θ_{bolts} (FEM)	θ_{bolts} (calculated)	(FEM/Calculated) (No Factor Applied)
2.00	2.74E-05	1.49E-05	1.84
2.25	2.65E-05	1.49E-05	1.78
2.38	2.62E-05	1.49E-05	1.76
2.50	2.59E-05	1.49E-05	1.74
2.75	2.53E-05	1.49E-05	1.70
3.00	2.49E-05	1.49E-05	1.67
Test 24-2-12:			
Thickness	θ_{bolts} (FEM)	θ_{bolts} (calculated)	(FEM/Calculated) (No Factor Applied)
1.75	2.48194E-05	2.00E-05	1.24
2	2.41944E-05	2.00E-05	1.21
2.25	2.36806E-05	2.00E-05	1.19
2.5	2.32917E-05	2.00E-05	1.17
2.75	2.29861E-05	2.00E-05	1.15

The additional factor is a result of plate and bolt flexibility. That flexibility tends to provide greater rotations compared to the simple model shown in figure 5.12.

5.4 Final Rotation Equation for an Annular Base Plate

The total rotation of the system was found to be a combination of plate and bolt rotation:

$$\theta_{total} = \theta_{plate} + \theta_{bolt} \tag{5-15}$$

Equations (5-9) and (5-14) were combined into equation (5-15) to quantify the resulting equation for the total rotation of an annular base plate.

$$\theta_{total} = \left[\frac{3M}{Er_b^2 b}\left(\frac{r_\Delta}{t_{plate}}\right)^3 + \frac{55M}{Er_b^2 b}\left(\frac{r_\Delta}{t_{plate}}\right)\right] + \left[\frac{1.5ML_b}{s_g A_b E_b r_b}\right] \tag{5-16}$$

where,

M = applied moment

E = modulus of elasticity

I_{plate} = estimated moment of inertia of the plate (calculated in Eqn (5-3))

r_Δ = distance between the edge of the pipe and the center of the bolt (rb-rp)

r_b = distance from the center of the pipe to the center of the bolt

A = effective area of the base plate

G = shear modulus

L_b = length of bolt under tension or compression

A_b = cross sectional area of bolt

E_b = modulus of elasticity of bolt

The results of equation (5-16) were compared to the results of the finite element analysis of the base plates, varying the thickness. The actual rotation of the base plate system was found by subtracting the deflection of the pipe from the overall deflection, then dividing by the length of the pipe. The results of that analysis are shown below in Table 5.12.

Table 5.12 Comparison of Actual Rotation to Predicted Rotation

Test 10-1-6:			
Thickness	Total Rotation (FEM)	Total Rotation (caluclated)	Calculated/ FEM
0.75	2.72E-03	2.73E-03	1.00
1	2.24E-03	2.47E-03	1.10
1.25	1.99E-03	2.33E-03	1.16
Test 25-2.375-8:			
Thickness	Total Rotation (FEM)	Total Rotation (caluclated)	Calculated/ FEM
2	9.09E-05	7.87E-05	0.86
2.25	7.77E-05	7.06E-05	0.91
2.375	7.21E-05	6.73E-05	0.93
2.5	6.72E-05	6.45E-05	0.96
2.75	5.90E-05	5.99E-05	1.01
3	5.25E-05	5.62E-05	1.07
Test 24-2-12:			
Thickness	Total Rotation (FEM)	Total Rotation (caluclated)	Calculated/ FEM
1.75	1.08E-04	1.00E-04	0.93
2	8.92E-05	8.88E-05	1.00
2.25	7.46E-05	8.06E-05	1.08
2.5	6.35E-05	7.46E-05	1.17
2.75	5.49E-05	6.98E-05	1.22

Equation (5-16) was also used to calculate the deflection of two typical FDOT mast arms due to the rotation of the annular base plate. The first mast arm evaluated,

pole 1, was used on FDOT project 25250-3523 in Alachua County, Florida at the intersection of S.R. 121 and 47th Avenue. The length of the mast arm used was 12.2 m. There was a 381-mm pipe with an inner wall thickness of 5 mm. The six-bolt plate configuration had a bolt diameter of 31.75 mm, an outer plate diameter of 535 mm, and a base plate thickness of 44.45 mm. A drawing of the mast arm and base plate can be seen below in Figure 5.13. The calculated deflection, using equation (5-16), due to the rotation of the annular base plate and bolts was 13.9 mm. The FEM deflection was 11.2 mm, differing by a factor of 0.81. The deflection of the mast arm, fixed at the base was determined to be 248.4 mm. The total deflection of a typical mast arm system, including the deflection from the annular base plate and anchor bolts was found to be 252.3 mm. The deflection due to the base plate and bolts made up 5.3% of the overall deflection of the mast arm system. Additionally, the deflection at the top of the pole was 28.5 mm, or 0.00158 m per 0.305 m. Since AASHTO (1994) allows 0.009 m of deflection per 0.305m of pole height, the mast arm is within specifications.

Additionally, pole 2, located at the same intersection as pole 1, was evaluated for overall deflection as well as deflection limitations. This mast arm had a base plate diameter of 635 mm, bolt diameter of 31.75 mm, and an arm length of 20.7 m, as shown in Figure 5.14. The overall deflection of the mast arm was 282.5 mm. Of that deflection, 12%, or 34.1 mm, came from the rotation of the base plate and bolts. The deflection at the top of the pole was 32.258 mm, or 0.00179 m per 0.305 m.

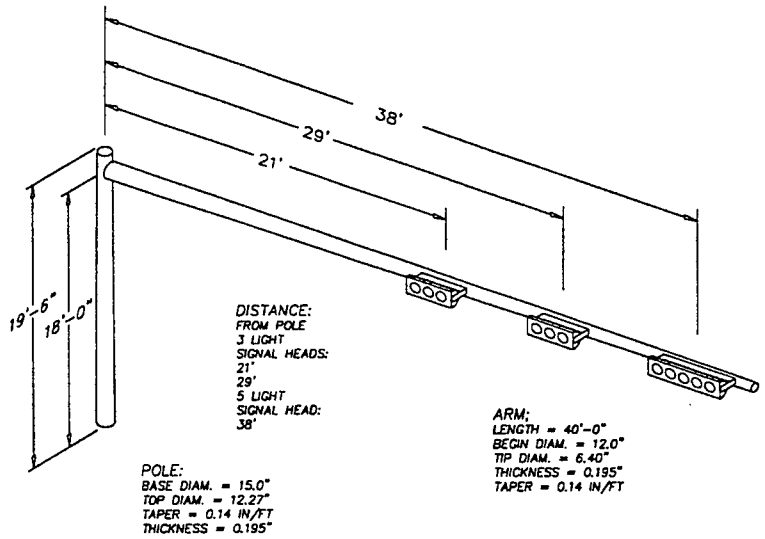

Figure 5.13 Pole 1 – FDOT Project 26250-3523

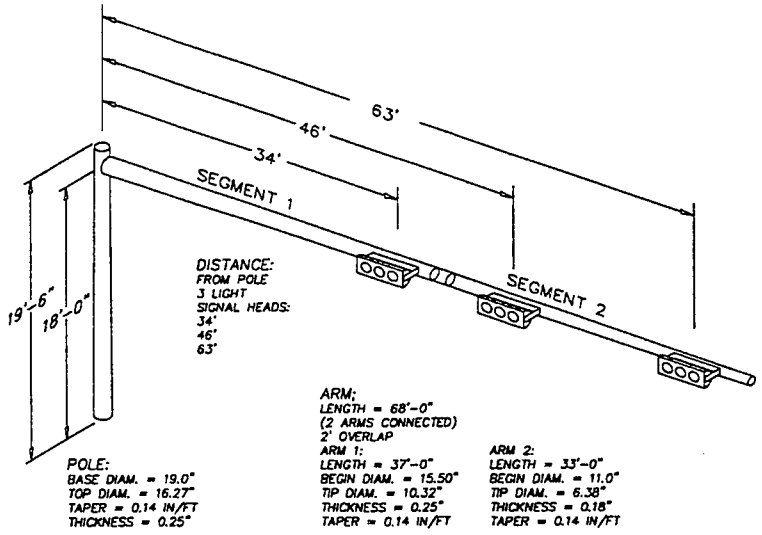

Figure 5.14 Pole 2 – FDOT Project 26250-3523

CHAPTER 6
SUMMARY AND CONCLUSIONS

6.1 Summary

Previous research performed by Cook et al. (1995) indicated that the rotational flexibility of an annular base plate connection (including flexibility's of the annular base plate and the anchor bolts) makes a significant contribution to the deflection of cantilevered mast-arm system systems. The purpose of the research presented in this report was to develop a design equation for predicting the rotation of the annular base plate connection.

In order to develop a design equation, a finite element program was used to analyze the annular base plate connection. A preprocessor to the finite element program, SSTAN (Hoit, 1995), was first written using Matlab. The finite element model was calibrated and its accuracy was verified by comparing the FEM results to the deflections found by the previous experimental tests (Cook et al., 1995). The model was then used to calculate rotations of typical FDOT base plates. A simple design equation based on basic engineering principles was developed. The design equation addressed both flexural and shear deformations in the base plate as well as axial deformations in the anchor bolts. The terms of the design equation were then calibrated to fit the results of the FEM results for typical FDOT base plates. In general, the calibration dealt with increasing the contribution of the term related to shear deformation of the base plate in order to account

for the flexibility of the pipe/plate socket weld. In typical FDOT applications, this joint tends to behave more as a pinned joint than a continuous member joint. The equation worked well within typical FDOT ranges.

6.2 Conclusions

Based on the results of this research, the following conclusions were made:

- Factors contributing to the rotation of the annular base plate connection were the rotation of the plate and the rotation caused by flexibility of the anchor bolts.
- The ratio of pipe thickness to plate thickness (t_{pipe}/t_{plate}) defines the manner in which the base plate deforms. Figure 5.3 demonstrates that when t_{pipe}/t_{plate} approaches 1, the pipe-plate interface remains at nearly 90°. As that ratio decreases, a hinge-like action occurs which causes the plate to undergo a rigid body "shear type" displacement as shown in Figure 5.2.
- The finite element analysis demonstrated that for typical FDOT connections, a shear-like deformation was occurring at the pipe/plate socket weld as shown in Figure 5.2.
- The final equation for plate rotation, Equation (5-10), consists of a rotation due to flexure and rotation due to shear. The equation is based on basic engineering principles but was calibrated with the FEM model to reflect the extreme "shear type" deformation caused by the pipe/plate socket weld.
- The final equation for connection rotation caused by axial flexibility of the anchor bolts is found in Equation (5-14). To properly model the connection rotation due to the bolts, a factor of 1.5 must be applied to the theoretical value given in Equation (5-

13). The 1.5 factor accounts for the concrete crushing that occurs at the embedded head of the anchor.

- Equation (5-16) provides the final design equation for calculating the rotation of annular base plate connections. The equation considers plate rotation, due to shear and flexure, combined with a rotation due to axial flexibility of the anchor bolts. Limitations on use of Equation (5-16) are presented in Chapter 5.
- For two typical FDOT mast arm systems the contribution of the rotation of the annular base plate connection to the tip deflection of the cantilevered mast arm was found to be less than 10%.

APPENDIX A
PREPROCESSOR TO SSTAN

```
I BATCH

fn='c:\Sstan\xlg10-3-6.inp';
Number_of_Bolts=10;
Radius_of_Pipe=18;
Thickness_of_Pipe=.575;
Radius_of_Plate=30;
Radius_of_Bolts=1.5;
Distance_to_Bolt_Center=24;
Num_Around_Bolt=5;
Num_Around_Plate=2;
Num_Radial_Cuts=4;
Num_cuts_on_side_of_bolt=1;
Thickness_of_Circles_Around_Bolt=.4;
Num_Around_Pipe=4;
Num_radial_cuts_in_bolt_section=1;
Num_layers_first_section_pipe=6;
Num_layers_second_section_pipe=4;
Num_layers_third_section_pipe=2;
Thickness_layer_1st_sect_pipe=3;
Thickness_layer_2nd_sect_pipe=5;
Thickness_layer_3rd_sect_pipe=17;
Thickness_of_base_plate=6;
Thickness_of_pipe=.575;

shift_angle=2*pi/20;
length_of_exposed_bolt=-1.5;
FX=0;
FY=1/10;
FZ=0;
MX=0;
MY=0;
MZ=0;
LC=1;
U=0.3;
E=29000;
NLC=1;
```

```
n_load1=1573;
n_load2=1609;
inc=4;

% Beam Properties
I21=337.7;
I31=337.7;
J1=675;
A1=49.5;
AS21=597;
AS31=597;
I22=3.377;
I32=3.377;
J2=6.75;
A2=1000;
AS22=597;
AS32=597;
```

II PIE

```
% PLATE  Calculates input mesh for base plate calculation
clear;
clear x;
clear y;
%format long;
batch;
n=Number_of_Bolts;
rp=Radius_of_Pipe;
tp=Thickness_of_Pipe;
rbp=Radius_of_Plate;
rb1=Radius_of_Bolts;
rb2=Distance_to_Bolt_Center;
cb=Num_Around_Bolt;
Cbplate=Num_Around_Plate;
c=Num_Radial_Cuts;
side_cuts=Num_cuts_on_side_of_bolt;
tcb=Thickness_of_Circles_Around_Bolt;
cp=Num_Around_Pipe;
rcut=Num_radial_cuts_in_bolt_section;
length=length_of_exposed_bolt;

%  Calculate size (angle)of each pie.
%  Calculate location (angle) for each bolt hole.

theta=2*pi/n;
```

```
mu=theta/c;

% Calculate (x,y) for Circle cuts around Pipe
% The addition and subtraction of mu is used as a spacer between circles around pipe
and bolt
% Rc is distance from center of pipe to last circle cut around pipe
Rc=cb*tcb+rb1+mu;
if Rc>rbp-rb2;
   Rc=rbp-rb2-mu;
end;
% Rp is distance from last circle cut around pipe to center of bolt
Rp=rb2-Rc-mu;
tcp=(Rp-rp)/cp;
% Loop to generate radial distance for each cut around pipe
j=0;
for j=1:cp;
 t=j*tcp;
 rcp=rp+t;
% Loop to generate nodes in increments of angle mu at each radial distance
 i=0;
 for alpha=0:mu:theta;
    i=i+1;
    pipex(i,1)=(rp-tp)*cos(alpha);
    pipey(i,1)=(rp-tp)*sin(alpha);
    pipex(i,2)=rp*cos(alpha);
    pipey(i,2)=rp*sin(alpha);
    pipex(i,2+j)=rcp*cos(alpha);
    pipey(i,2+j)=rcp*sin(alpha);
 end;
end;



% Calculate (x,y) for Circle cuts around the inside edge of Base Plate
% Rbplate is radial distance for first cut around inside of base plate
% tbplate is distance between each cut
Rbplate=Rp+2*Rc+mu;
tbplate=(rbp-Rbplate)/(Cbplate-1);
j=0;
for j=1:Cbplate;
 t=j*tbplate-tbplate;
 rcbplate=Rbplate+t+mu;
 i=0;
 for alpha=0:mu:theta;
    i=i+1;
```

```
      bpx(i,j)=rcbplate*cos(alpha);
      bpy(i,j)=rcbplate*sin(alpha);
    end;
  end;

  % Cuts around the bolts
  % The bolt is broken into four quadrants
  % In addition to the quadrants that create nodes in a circle-like pattern around the bolt, %
  % there are nodes formed in a radial pattern in between the bolts
  % Format the radial nodes on the left side of the bolt
  % nincr determines the number of nodes to generate along radial lines
  % L1 is the span in which these nodes will be distributed evenly
  nincr=2*rcut+side_cuts;
  L1=Rbplate-Rp;
  j=0;
  % First loop generates nodes at an incremented amount along the radial line
  % Second loop generates these nodes at specific angles
  for j=1:nincr;
     i=0;
     for alpha=0:mu:mu*rcut;
        i=i+1;
        incrxr3=L1*cos(alpha)/nincr;
           incryr3=L1*sin(alpha)/nincr;
           Rpx=Rp*cos(alpha);
           Rpy=Rp*sin(alpha);
           Jx(i,j)=Rpx+incrxr3*j;
           Jy(i,j)=Rpy+incryr3*j;
    end;
  end;

  % Format the radial nodes on the right side of the bolt

  j=0;
  for j=1:nincr;
     i=0;
     for alpha=(c-rcut)*mu:mu:theta;
        i=i+1;
        incrxr4=L1*cos(alpha)/nincr;
           incryr4=L1*sin(alpha)/nincr;
           Rpx=Rp*cos(alpha);
           Rpy=Rp*sin(alpha);
           Kx(i,j)=Rpx+incrxr4*j;
           Ky(i,j)=Rpy+incryr4*j;
    end;
  end;
```

```
% Calculate the Section around the bolts;
% Ax and Ay calculate the coordinates of the center of the bolt
gamma=0;
Ax=rb2*cos(theta/2);
Ay=rb2*sin(theta/2);

% Quadrant I
% Quadrant I is the section in between the pipe and the bolt
% Br3x, Br3y calculates coordinates of first node that creates circle pattern in Quadrant I
for i=1:rcut;
   beta=mu*rcut;
   Br3x=Rp*cos(beta)+L1*cos(beta)/nincr*(rcut+1-i);
   Br3y=Rp*sin(beta)+L1*sin(beta)/nincr*(rcut+1-i);
   deltax=abs(Ax-Br3x);
   deltay=abs(Ay-Br3y);
   phi=atan(deltay/deltax);
   rb1x=rb1*cos(phi);
   rb1y=rb1*sin(phi);
   tcbx=tcb*cos(phi);
   tcby=tcb*sin(phi);
   j=0;
   for j=1:cb;
        if Ax>Br3x;
        C1x(i,1)=Ax-rb1x;
        C1x(i,1+j)=Ax-tcbx*j-rb1x;
        elseif Ax<Br3x;
        C1x(i,1)=Ax+rb1x;
        C1x(i,1+j)=Ax+tcbx*j+rb1x;
        end;
        if Ay>Br3y;
        C1y(i,1)=Ay-rb1y;
        C1y(i,1+j)=Ay-tcby*j-rb1y;
        elseif Ay<Br3y;
        C1y(i,1)=Ay+rb1y;
        C1y(i,1+j)=Ay+tcby*j+rb1y;
        end;
   end;
end;
i=0;
for alpha=mu*rcut:mu:(mu*rcut+(c-2*rcut)*mu);
   i=i+1;
   Bx=Rp*cos(alpha);
   By=Rp*sin(alpha);
   deltax=abs(Ax-Bx);
```

```
    deltay=abs(Ay-By);
    phi=atan(deltay/deltax);
    rb1x=rb1*cos(phi);
    rb1y=rb1*sin(phi);
    if Ax>Bx;
    Cx(i,1)=Ax-rb1x;
    elseif Ax<Bx;
    Cx(i,1)=Ax+rb1x;
    end;
    if Ay>By;
    Cy(i,1)=Ay-rb1y;
    elseif Ay<By;
    Cy(i,1)=Ay+rb1y;
    end;
    tcbx=tcb*cos(phi);
    tcby=tcb*sin(phi);
    j=0;
%cuts around bolt;
    for j=1:cb;
      if Ax>Bx;
        Cx(i,1+j)=Ax-tcbx*j-rb1x;
      elseif Ax<Bx;
        Cx(i,1+j)=Ax+tcbx*j+rb1x;
      end;
      if Ay>By;
        Cy(i,1+j)=Ay-tcby*j-rb1y;
      elseif Ay<By;
        Cy(i,1+j)=Ay+tcby*j+rb1y;
      end;
    end;
end;
for i=1:rcut;
    beta=mu*rcut+(c-2*rcut)*mu;
    Br3x=Rp*cos(beta)+L1*cos(beta)/nincr*i;
    Br3y=Rp*sin(beta)+L1*sin(beta)/nincr*i;
    deltax=abs(Ax-Br3x);
    deltay=abs(Ay-Br3y);
    phi=atan(deltay/deltax);
    rb1x=rb1*cos(phi);
    rb1y=rb1*sin(phi);
    tcbx=tcb*cos(phi);
    tcby=tcb*sin(phi);
    for j=1:cb;
        if Ax>Br3x;
        C2x(i,1)=Ax-rb1x;
```

```
        C2x(i,1+j)=Ax-tcbx*j-rb1x;
        elseif Ax<Br3x;
        C2x(i,1)=Ax+rb1x;
        C2x(i,1+j)=Ax+tcbx*j+rb1x;
        end;
        if Ay>Br3y;
        C2y(i,1)=Ay-rb1y;
        C2y(i,1+j)=Ay-tcby*j-rb1y;
        elseif Ay<Br3y;
        C2y(i,1)=Ay+rb1y;
        C2y(i,1+j)=Ay+tcby*j+rb1y;
        end;
    end;
end;

%Quadrant II;
for i=1:rcut;
    beta=mu*rcut+(c-2*rcut)*mu;
    Br4x=Rp*cos(beta)+L1*cos(beta)/nincr*(nincr+1-i);
    Br4y=Rp*sin(beta)+L1*sin(beta)/nincr*(nincr+1-i);
    deltax=abs(Ax-Br4x);
    deltay=abs(Ay-Br4y);
    phi=atan(deltay/deltax);
    rb1x=rb1*cos(phi);
    rb1y=rb1*sin(phi);
    tcbx=tcb*cos(phi);
    tcby=tcb*sin(phi);
    j=0;
    for j=1:cb;
        if Ax>Br4x;
        E1x(i,1)=Ax-rb1x;
        E1x(i,1+j)=Ax-tcbx*j-rb1x;
        elseif Ax<Br4x;
        E1x(i,1)=Ax+rb1x;
        E1x(i,1+j)=Ax+tcbx*j+rb1x;
        end;
        if Ay>Br4y;
        E1y(i,1)=Ay-rb1y;
        E1y(i,1+j)=Ay-tcby*j-rb1y;
        elseif Ay<Br4y;
        E1y(i,1)=Ay+rb1y;
        E1y(i,1+j)=Ay+tcby*j+rb1y;
        end;
    end;
end;
```

```
i=0;
for alpha=mu*rcut:mu:(mu*rcut+(c-2*rcut)*mu);
   i=i+1;
   Dx=(Rbplate+mu)*cos(alpha);
   Dy=(Rbplate+mu)*sin(alpha);
   deltax=abs(Ax-Dx);
   deltay=abs(Ay-Dy);
   phi=atan(deltay/deltax);
   rb1x=rb1*cos(phi);
   rb1y=rb1*sin(phi);
   if Ax>Dx;
      Ex(i,1)=Ax-rb1x;
   elseif Ax<Dx;
      Ex(i,1)=Ax+rb1x;
   end;
   if Ay>Dy;
      Ey(i,1)=Ay-rb1y;
   elseif Ay<Dy;
      Ey(i,1)=Ay+rb1y;
   end;
   tcbx=tcb*cos(phi);
   tcby=tcb*sin(phi);
   j=0;
%cuts around bolt;
   for j=1:cb;
      if Ax>Dx;
        Ex(i,1+j)=Ax-tcbx*j-rb1x;
      elseif Ax<Dx;
        Ex(i,1+j)=Ax+tcbx*j+rb1x;
      end;
      if Ay>Dy;
        Ey(i,1+j)=Ay-tcby*j-rb1y;
      elseif Ay<Dy;
        Ey(i,1+j)=Ay+tcby*j+rb1y;
      end;
   end;
end;
for i=1:rcut;
   beta=mu*rcut;
   Br4x=Rp*cos(beta)+L1*cos(beta)/nincr*(nincr-rcut+i);
   Br4y=Rp*sin(beta)+L1*sin(beta)/nincr*(nincr-rcut+i);
   deltax=abs(Ax-Br4x);
   deltay=abs(Ay-Br4y);
   phi=atan(deltay/deltax);
   rb1x=rb1*cos(phi);
```

```
    rb1y=rb1*sin(phi);
    tcbx=tcb*cos(phi);
    tcby=tcb*sin(phi);
    j=0;
    for j=1:cb;
        if Ax>Br4x;
        E2x(i,1)=Ax-rb1x;
        E2x(i,1+j)=Ax-tcbx*j-rb1x;
        elseif Ax<Br4x;
        E2x(i,1)=Ax+rb1x;
        E2x(i,1+j)=Ax+tcbx*j+rb1x;
        end;
        if Ay>Br4y;
        E2y(i,1)=Ay-rb1y;
        E2y(i,1+j)=Ay-tcby*j-rb1y;
        elseif Ay<Br4y;
        E2y(i,1)=Ay+rb1y;
        E2y(i,1+j)=Ay+tcby*j+rb1y;
        end;
    end;
end;


%Quadrant III;
for i=1:side_cuts;
    beta=mu*rcut;
    Fx=Rp*cos(beta)+L1*cos(beta)/nincr*(rcut+i);
    Fy=Rp*sin(beta)+L1*sin(beta)/nincr*(rcut+i);
    deltax=abs(Ax-Fx);
    deltay=abs(Ay-Fy);
    phi=atan(deltay/deltax);
    rb1x=rb1*cos(phi);
    rb1y=rb1*sin(phi);
    tcbx=tcb*cos(phi);
    tcby=tcb*sin(phi);
    j=0;
    for j=1:cb;
        if Ax>Fx;
        Gx(i,1)=Ax-rb1x;
        Gx(i,1+j)=Ax-tcbx*j-rb1x;
        elseif Ax<Fx;
        Gx(i,1)=Ax+rb1x;
        Gx(i,1+j)=Ax+tcbx*j+rb1x;
        end;
        if Ay>Fy;
```

```
        Gy(i,1)=Ay-rb1y;
        Gy(i,1+j)=Ay-tcby*j-rb1y;
        elseif Ay<Fy;
        Gy(i,1)=Ay+rb1y;
        Gy(i,1+j)=Ay+tcby*j+rb1y;
        end;
   end;
end;


%Quadrant IV;
for i=1:side_cuts;
   beta=mu*rcut+(c-2*rcut)*mu;
   Hx=Rp*cos(beta)+L1*cos(beta)/nincr*(rcut+i);
   Hy=Rp*sin(beta)+L1*sin(beta)/nincr*(rcut+i);
   deltax=abs(Ax-Hx);
   deltay=abs(Ay-Hy);
   phi=atan(deltay/deltax);
   rb1x=rb1*cos(phi);
   rb1y=rb1*sin(phi);
   tcbx=tcb*cos(phi);
   tcby=tcb*sin(phi);
   j=0;
   for j=1:cb;
        if Ax>Hx;
        Ix(i,1)=Ax-rb1x;
        Ix(i,1+j)=Ax-tcbx*j-rb1x;
        elseif Ax<Hx;
        Ix(i,1)=Ax+rb1x;
        Ix(i,1+j)=Ax+tcbx*j+rb1x;
        end;
        if Ay>Hy;
        Iy(i,1)=Ay-rb1y;
        Iy(i,1+j)=Ay-tcby*j-rb1y;
        elseif Ay<Hy;
        Iy(i,1)=Ay+rb1y;
        Iy(i,1+j)=Ay+tcby*j+rb1y;
        end;
   end;
end;

% Format Matrices for x & y coordinates
% Combines the coordinates from each quadrant to form matrices for x and y
coordinates
m1c=size(C1x);
```

```
mc=size(Cx);
m2c=size(C2x);
mi=size(Ix);
m1e=size(E1x);
me=size(Ex);
m2e=size(E2x);
mg=size(Gx);
for j=1:cb+1;
   for i=1:m1c(1);
      boltx(i,j)=C1x(i,j);
      bolty(i,j)=C1y(i,j);
   end;
   for i=1:mc(1);
      boltx(i+m1c(1),j)=Cx(i,j);
      bolty(i+m1c(1),j)=Cy(i,j);
   end;
   for i=1:m2c(1);
      boltx(i+m1c(1)+mc(1),j)=C2x(i,j);
      bolty(i+m1c(1)+mc(1),j)=C2y(i,j);
   end;
   for i=1:mi(1);
      boltx(i+m1c(1)+mc(1)+m2c(1),j)=Ix(i,j);
      bolty(i+m1c(1)+mc(1)+m2c(1),j)=Iy(i,j);
   end;
   for i=1:m1e(1);
      boltx(i+mi(1)+m2c(1)+mc(1)+m1c(1),j)=E1x(m1e(1)-i+1,j);
      bolty(i+mi(1)+m2c(1)+mc(1)+m1c(1),j)=E1y(m1e(1)-i+1,j);
   end;
   for i=1:me(1);
      boltx(i+m1e(1)+mi(1)+m2c(1)+mc(1)+m1c(1),j)=Ex(me(1)-i+1,j);
      bolty(i+m1e(1)+mi(1)+m2c(1)+mc(1)+m1c(1),j)=Ey(me(1)-i+1,j);
   end;
   for i=1:m2e(1);
      boltx(i+me(1)+m1e(1)+mi(1)+m2c(1)+mc(1)+m1c(1),j)=E2x(m2e(1)-i+1,j);
      bolty(i+me(1)+m1e(1)+mi(1)+m2c(1)+mc(1)+m1c(1),j)=E2y(m2e(1)-i+1,j);
   end;
   for i=1:mg(1);
      boltx(i+m2e(1)+me(1)+m1e(1)+m2c(1)+mc(1)+m1c(1)+mi(1),j)=Gx(mg(1)-i+1,j);
      bolty(i+m2e(1)+me(1)+m1e(1)+m2c(1)+mc(1)+m1c(1)+mi(1),j)=Gy(mg(1)-i+1,j);
   end;
end;

% Format for section around the pipe;
% Shows the Element numbers corresponding to specific nodes
NEL1=(floor(cp)+1)*c;
```

```
NEL3=NEL1+(Cbplate-1)*c;
nt=c+1;
% Format for elements within the pipe region
% The element matrice is in form of element number, node 1, node 2, node 3, node 4
for el=1:NEL1;
   m1=el/c;
   Element(el,1)=el;
   Element(el,2)=el+ceil(m1)-1;
   Element(el,3)=el+ceil(m1);
   Element(el,4)=el+nt+ceil(m1)-1;
   Element(el,5)=el+nt+ceil(m1);
end;
% Format for elements within the base plate region
for el=(NEL1+1):NEL3;
   m3=el/c;
   Element(el,1)=el;
   Element(el,2)=el+c+ceil(m3);
   Element(el,3)=el+c+ceil(m3)+1;
   Element(el,4)=el+c+nt+ceil(m3);
   Element(el,5)=el+c+nt+ceil(m3)+1;
end;
% Format for elements contained in Quadrant 3, radial region
last_node=Element(NEL3,5);
diff=last_node-NEL3;
for j=1;
   for i=1:rcut;
         el=NEL3+i;
         Element(el,1)=el;
         Element(el,2)=Element(el-c*Cbplate,4);
    Element(el,3)=Element(el-c*Cbplate,5);
    Element(el,4)=el+diff;
    Element(el,5)=el+diff+1;
   end;
end;
for j=1:nincr-1;
   for i=1:rcut;
         el=NEL3+rcut*j+i;
         Element(el,1)=el;
         Element(el,2)=el+diff-rcut-1+j;
    Element(el,3)=el+diff-rcut+j;
    Element(el,4)=el+diff+j;
    Element(el,5)=el+diff+1+j;
   end;
end;
melement=size(Element);
```

```
last_element=melement(1);
for j=1;
  for i=1:rcut;
       el=last_element+i;
       Element(el,1)=el;
       Element(el,2)=el+diff+rcut;
   Element(el,3)=el+diff+rcut+1;
   Element(el,4)=Element(el-rcut*nincr-c*(Cbplate-1),2);
   Element(el,5)=Element(el-rcut*nincr-c*(Cbplate-1),3);
  end;
end;
% Format for elements contained in Quadrant 4, radial region
melement=size(Element);
last_element=melement(1);
last_node=Element(last_element,3);
for j=1;
  for i=1:rcut;
       el=last_element+i;
       Element(el,1)=el;
       Element(el,2)=Element(el-(1+nincr)*rcut-c*(Cbplate-1)-rcut,4);
   Element(el,3)=Element(el-(1+nincr)*rcut-c*(Cbplate-1)-rcut,5);
   Element(el,4)=last_node+i;
   Element(el,5)=last_node+i+1;
  end;
end;
diff=(last_node+1)-(last_element+rcut+1);
for j=1:nincr-1;
  for i=1:rcut;
       el=last_element+rcut*j+i;
       Element(el,1)=el;
       Element(el,2)=el+diff+j-1;
   Element(el,3)=el+diff+j;
   Element(el,4)=el+diff+j+rcut;
   Element(el,5)=el+diff+j+rcut+1;
  end;
end;
melement=size(Element);
last_element=melement(1);
for j=1;
  for i=1:rcut;
       el=last_element+i;
       Element(el,1)=el;
       Element(el,2)=el+diff+nincr-1;
   Element(el,3)=el+diff+nincr;
   Element(el,4)=Element(el-(2*rcut*nincr+rcut)-rcut,2);
```

```
    Element(el,5)=Element(el-(2*rcut*nincr+rcut)-rcut,3);
  end;
end;
% Format for Elements arount the bolt
mbolt=size(boltx);
diff=Element(last_element+rcut,3)-(last_element+rcut);
for j=1:cb+1;
  for i=1:mbolt(1);
      el=last_element+rcut+i+mbolt(1)*(j-1);
      Element(el,1)=el;
      Element(el,2)=el+diff;
      Element(el,3)=el+diff+1;
      Element(el,4)=el+diff+mbolt(1);
      Element(el,5)=el+diff+mbolt(1)+1;
  end;
end;
for i=1:cb;
  el=last_element+rcut+mbolt(1)*i;
  Element(el,3)=el-mbolt(1)+1+diff;
  Element(el,5)=el-mbolt(1)+1+diff+mbolt(1);
end;
for i=1:rcut;
  el=last_element+rcut+mbolt(1)*cb+i;
  Element(el,4)=Element(NEL3+rcut*(rcut+1-i),5);
  Element(el,5)=Element(NEL3+rcut*(rcut+1-i),3);
end;
for i=1:c-2*rcut;
  el=last_element+rcut+mbolt(1)*cb+rcut+i;
  Element(el,4)=Element(NEL1-rcut-(c-2*rcut)+i,4);
  Element(el,5)=Element(NEL1-rcut-(c-2*rcut)+i,5);
end;
for i=1:nincr+1;
  el=last_element+rcut+mbolt(1)*cb+rcut+(c-2*rcut)+i;
  Element(el,4)=Element(NEL3+rcut*(nincr+1)+rcut*(i-1)+1,2);
  Element(el,5)=Element(NEL3+rcut*(nincr+1)+rcut*(i-1)+1,4);
end;
for i=1:c-2*rcut;
  el=last_element+rcut+mbolt(1)*cb+rcut+(c-2*rcut)+nincr+1+i;
  Element(el,4)=Element(NEL3-rcut+1-i,3);
  Element(el,5)=Element(NEL3-rcut+1-i,2);
end;
for i=1:rcut+side_cuts+1;
  el=last_element+rcut+mbolt(1)*cb+rcut+(c-2*rcut)+nincr+1+c-2*rcut+i;
  Element(el,4)=Element(NEL3+rcut*rcut+rcut*(rcut+side_cuts+2-i),5);
  Element(el,5)=Element(NEL3+rcut*rcut+rcut*(rcut+side_cuts+2-i),3);
```

```
end;
mel=size(Element);
el=mel(1);
Element(el,3)=Element(el-mbolt(1)+1,2);

% Format for Nodes and their corresponding coordinates
%  Matrice Nodes is in form of Node Number, x-coordinate, y-coordinate, z-coordinate
% Format for Nodes in the pipe region
mpipe=size(pipex);
k=0;
for j=1:mpipe(2);
   for i=1:mpipe(1);
      k=k+1;
      Node(k,1)=k;
      Node(k,2)=pipex(i,j);
      Node(k,3)=pipey(i,j);
          Node(k,4)=0;
   end;
end;
% Format for Nodes in the base plate region
mbp=size(bpx);
for j=1:mbp(2);
   for i=1:mbp(1);
      k=k+1;
      Node(k,1)=k;
      Node(k,2)=bpx(i,j);
      Node(k,3)=bpy(i,j);
          Node(k,4)=0;
   end;
end;
% Format for Nodes in Quadrant III bolt region
mrbolt3=size(Jx);
for j=1:mrbolt3(2);
   for i=1:mrbolt3(1);
         k=k+1;
         Node(k,1)=k;
         Node(k,2)=Jx(i,j);
         Node(k,3)=Jy(i,j);
         Node(k,4)=0;
   end;
end;
% Format for Nodes in Quadrant IV bolt region
mrbolt4=size(Kx);
for j=1:mrbolt4(2);
   for i=1:mrbolt4(1);
```

```
        k=k+1;
        Node(k,1)=k;
        Node(k,2)=Kx(i,j);
        Node(k,3)=Ky(i,j);
        Node(k,4)=0;
   end;
end;
% Format for Nodes in the bolt region
mbolt=size(boltx);
for j=1:mbolt(2);
   for i=1:mbolt(1);
      k=k+1;
      Node(k,1)=k;
      Node(k,2)=boltx(i,j);
      Node(k,3)=bolty(i,j);
        Node(k,4)=0;
   end;
end;

% Sets very small numbers to zero
num_nodes=size(Node);
for i=1:num_nodes(1);
   for j=2:num_nodes(2);
        if Node(i,j)<0.00000000001;
          Node(i,j)=0;
        end;
   end;
end;
```

III PLATE

```
% The routine, PLATE, runs pie, sorts the nodes based on their coordinates, and copies
%them to other pie pieces to form the entire plate. The nodes along the edges of the pie
%are not counted twice. The purposes of the sort and swap routines are to rename the
%nodes on the edge of one pie piece, using the largest node numbers in that pie section.
%Consequently, those large numbered nodes make up the first group of nodes for the
%next section.
% Following lines call the subroutines batch and pie
batch
pie

n_node=size(Node);
m_ele=size(Element);

% Sorts by lowest y values
```

```
for j=1:n_node(1);
   for i=1:n_node(1)-1;

      if Node(i,3)>Node(i+1,3);
         buff1=Node(i,:);
         Node(i,:)=Node(i+1,:);
         Node(i+1,:)=buff1;
      end;
   end;
end;

%  Counts number of zero y values

i=1;
while Node(i,3)<=0;
   Node(i,3)=0;
   i=i+1;
end;
num=i-1;

% Sorts by lowest x values for zero y values

for j=1:num;
   for i=1:num-1;
      if Node(i,2)>Node(i+1,2);
         buff=Node(i,:);
         Node(i,:)=Node(i+1,:);
         Node(i+1,:)=buff;
      end;
   end;
end;

%  Swaps Node numbers in Node and Element

for j=1:num;
   buff=Node(j,1);
   for i=1:n_node(1);
      if Node(i,1)==j;
         Node(j,1)=j;
         Node(i,1)=buff;
         for k=1:m_ele(1);
            for l=2:5;
               if Element(k,l)==j;
                  Element(k,l)=buff;
```

```
            elseif Element(k,l)==buff;
               Element(k,l)=j;
            end;
         end;
      end;
   end;
end;

Node=phase(Node,-theta);

% Sorts by lowest y values

for j=1:n_node(1);
   for i=1:n_node(1)-1;
      if Node(i,3)<Node(i+1,3);
         buff=Node(i,:);
         Node(i,:)=Node(i+1,:);
         Node(i+1,:)=buff;
      end;
   end;
end;

% Sets very small numbers to zero
num_nodes=size(Node);
for i=1:num_nodes(1);
   for j=2:num_nodes(2);
        if Node(i,j)<0.00000000001&Node(i,j)>-0.00000000001;
          Node(i,j)=0;
        end;
   end;
end;

%  Counts number of zero y values

i=1;
while Node(i,3)==0;
   Node(i,3)=0;
   i=i+1;
end;
num=i-1;

% Sorts by highest x values for zero y values

for j=1:num;
```

```
   for i=1:num-1;
      if Node(i,2)<Node(i+1,2);
         buff=Node(i,:);
         Node(i,:)=Node(i+1,:);
         Node(i+1,:)=buff;
      end;
   end;
end;


% Swaps Node numbers in Node and Element

for j=1:num;
   buff=Node(j,1);
   for i=1:n_node(1);
      if Node(i,1)==n_node(1)-j+1;
         Node(j,1)=n_node(1)-j+1;
         Node(i,1)=buff;
         for k=1:m_ele(1);
            for l=2:5;
               if Element(k,l)==n_node(1)-j+1;
                  Element(k,l)=buff;
               elseif Element(k,l)==buff;
                  Element(k,l)=n_node(1)-j+1;
               end;
            end;
         end;
      end;
   end;
end;

Node=phase(Node,theta);

% Sorts by lowest y values

for j=1:n_node(1);
   for i=1:n_node(1)-1;
      if Node(i,1)>Node(i+1,1);
         buff=Node(i,:);
         Node(i,:)=Node(i+1,:);
         Node(i+1,:)=buff;
      end;
   end;
end;
```

```
node_num=n_node(1);
element_num=m_ele(1);
for i=1:n-1;
   gamma=theta*i;
   node_buff=phase(Node(1:n_node(1),:),gamma);
   element_buff(1:m_ele(1),:)=Element(1:m_ele(1),:);
   for j=1:n_node(1);
      node_buff(j,1)=node_buff(j,1)+(n_node(1)-num)*i;
   end;
   for j=1:m_ele(1);
      element_buff(j,1)=j+i*m_ele(1);
      for k=2:5;
         element_buff(j,k)=element_buff(j,k)+(n_node(1)-num)*i;
      end;
   end;
   for j=1:n_node(1)-num;
       node_num=node_num+1;
       Node(node_num,:)=node_buff(j+num,:);
   end;
   for j=1:m_ele(1);
      element_num=element_num+1;
      Element(element_num,:)=element_buff(j,:);
   end;
end;

n_node=size(Node);
m_ele=size(Element);
for j=n_node(1)-num+1:n_node(1);
   for i=1:m_ele(1);
      for k=2:5;
         if Element(i,k)==Node(j,1);
            Element(i,k)=Node(j-n_node(1)+num,1);
         end;
      end;
   end;
end;

buff=Node;
clear Node;
Node(1:n_node-num(1),:)=buff(1:n_node(1)-num,:);

% Determines the nodes located around the bolt
Num_Nodes=size(Node);
num_per_bolt=Num_Nodes(1)/n;
num_in_bolt=2*((c+1)+side_cuts);
```

```
i=0;
for j=1:num_in_bolt;
i=i+1;
  nbolt(i,1)=(c+1)*(cp+2)+(c+1)*(Cbplate)+2*(rcut+1)*nincr+i;
end;

node1=nbolt(1,1);

for k=1:n-1;
  for j=1:num_in_bolt;
i=i+1;
        nbolt(i,1)=node1+num_per_bolt*k+j-1;
  end;
end;
melements=size(Element);
mnodes=size(Node);

pipe;

i=lastnode2(1);
j=lastnode2(1);
for alpha=theta/2:theta:2*pi-theta/2;
   i=i+1;
   j=j+1;
   Node(i,1)=j;
   Node(i,2)=rb2*cos(alpha);
   Node(i,3)=rb2*sin(alpha);
   Node(i,4)=0;
end;

% Adds Coordinates to Create Beam Elements to Model the Bolts

for alpha=theta/2:theta:2*pi-theta/2;
   i=i+1;
   j=j+1;
   Node(i,1)=j;
   Node(i,2)=rb2*cos(alpha);
   Node(i,3)=rb2*sin(alpha);
   Node(i,4)=length;
end;

Node=phase(Node,shift_angle);

i=i+1;
```

```
Node(i,1)=j+1;
Node(i,2)=0;
Node(i,3)=0;
Node(i,4)=length;

% Creates Matrix for Beam Elements to Model Bolts
nelem=size(Element);
l_nodeb=size(Node);
i=0;
k=0;
numbolt=size(nbolt);
NMB=numbolt(1)+n;
npb=numbolt(1)/n;
for k=1:n;
   for j=1:numbolt(1)/n;
        i=i+1;
        bolt(i,1)=nelem(1)+npb*(k-1)+j;
        bolt(i,2)=nbolt(i,1);
        bolt(i,3)=lastnode2(1)+k;
        bolt(i,4)=l_nodeb(1);
   end;
end;
k=0;
l=0;
for j=1:n;
   i=i+1;
   k=k+1;
   l=l+1;
   bolt(i,1)=nelem(1)+n*npb+j;
   bolt(i,2)=lastnode2(1)+k;
   bolt(i,3)=lastnode2(1)+n+l;
   bolt(i,4)=l_nodeb(1);
end;
```

sstan

IV PIPE

% Pipe allows the users to create three levels of pipe section at different heights and %thicknesses. The nodes and elements created in this section are added to the matrices %NODE and ELEMENT.

```
c1=Num_layers_first_section_pipe;
c2=Num_layers_second_section_pipe;
c3=Num_layers_third_section_pipe;
t1=Thickness_layer_1st_sect_pipe;
t2=Thickness_layer_2nd_sect_pipe;
t3=Thickness_layer_3rd_sect_pipe;

radius=Node;
r=size(Node);
for i=1:r(1);
   radius(i,5)=sqrt((radius(i,2))^2+(radius(i,3))^2);
end;

% Sorts Node numbers in radius to find nodes along bottom of pipe;

for j=1:r(1);
   for i=1:r(1)-1;
         if radius(i,5)>radius(i+1,5);
            buff=radius(i,:);
            radius(i,:)=radius(i+1,:);
            radius(i+1,:)=buff;
         end;
   end;
end;
radius1=radius;

% Counts number of nodes along pipe

buff=radius(1,5);
num=2;
while round(100000*radius(num,5))==round(100000*buff);
   num=num+1;
end;
num=num-1;

% Sorts Node numbers in proper order
for j=1:num;
   for i=1:num-1;
         if radius(i,3)<radius(i+1,3);
            buff=radius(i,:);
            radius(i,:)=radius(i+1,:);
            radius(i+1,:)=buff;
         end;
   end;
end;
```

```
for j=1:num/2+1;
   for i=1:num/2;
        if radius(i,2)<radius(i+1,2)
          buff=radius(i,:);
          radius(i,:)=radius(i+1,:);
          radius(i+1,:)=buff;
        end;
   end;
end;
for j=num/2+2:num;
   for i=num/2+2:num-1;
        if radius(i,2)>radius(i+1,2)
          buff=radius(i,:);
          radius(i,:)=radius(i+1,:);
          radius(i+1,:)=buff;
        end;
   end;
end;


lastnode1=size(radius);

%  Swaps Node numbers in Node and Element

Node=radius(:,1:5);

n_node=size(Node);
m_ele=size(Element);
for j=1:num;
   buff=Node(j,1);
   for i=1:n_node(1);
      if Node(i,1)==j;
        Node(j,1)=j;
        Node(i,1)=buff;
        for k=1:m_ele(1);
          for l=2:5;
            if Element(k,l)==j;
              Element(k,l)=buff;
            elseif Element(k,l)==buff;
              Element(k,l)=j;
            end;
          end;
        end;
      end;
   end;
```

```
end;

Node=sort1(Node,1,1);

% Creates the Nodes for the pipe

k=0;
for j=1:c1;
   for k=1:num;
        i=i+1;
        Node(i,1)=i;
        Node(i,2)=Node(k,2);
        Node(i,3)=Node(k,3);
        Node(i,4)=t1*j;
   end;
end;

for j=1:c2;
   for k=1:num;
        i=i+1;
        Node(i,1)=i;
        Node(i,2)=Node(k,2);
        Node(i,3)=Node(k,3);
        Node(i,4)=t1*c1+t2*j;
   end;
end;

for j=1:c3;
   for k=1:num;
        i=i+1;
        Node(i,1)=i;
        Node(i,2)=Node(k,2);
        Node(i,3)=Node(k,3);
        Node(i,4)=t1*c1+t2*c2+t3*j;
   end;
end;

% Creates pipe elements

layer=c1+c2+c3;
for j=1:layer-1;
   for i=1:num;
        el=m_ele(1)+j*num+i;
        Element(el,1)=el;
        Element(el,2)=n_node(1)+(j-1)*num+i;
```

```
        Element(el,3)=n_node(1)+(j-1)*num+i+1;
        Element(el,4)=n_node(1)+j*num+i;
        Element(el,5)=n_node(1)+j*num+i+1;
   end;
end;
% Creates elements on bottom row of pipe
for i=1:num;
        el=m_ele(1)+i;
        Element(el,1)=el;
        Element(el,2)=i;
        Element(el,3)=i+1;
        Element(el,4)=n_node(1)+i;
        Element(el,5)=n_node(1)+i+1;
end;
el=m_ele(1)+num;
elem=m_ele(1)+1;
Element(el,3)=Element(elem,2);
Element(el,5)=Element(elem,4);
% Creates elements in the last row of pipe
for j=1:layer-1;
        el=m_ele(1)+(j+1)*num;
        Element(el,3)=n_node(1)+(j-1)*num+1;
        Element(el,5)=n_node(1)+j*num+1;
end;

lastnode2=size(Node);
melements2=size(Element);
```

V PHASE

```
% The purpose of this subroutine is to shift the plate over by a certain angle. This allows
%the user more variety to analyze the base plate. This routine may be ommitted by
%deleting the line, Node=phase(Node,shift_angle);, that is placed toward the end of the
%the routine, PLATE.


function Node=phase(Node,delta_angle)
% PHASE shifts Node through delta_angle radians

n=size(Node);

for i=1:n(1);
   x=Node(i,2);
   y=Node(i,3);
   z=Node(i,4);
```

```
   r=sqrt(x^2+y^2);
   if x>=0 & y >=0;
        angle=asin(y/r);
   elseif x<0 & y>=0;
        angle=pi-asin(y/r);
   elseif x<0 & y<0;
        angle=pi-asin(y/r);
   elseif x>=0 & y<0;
        angle=2*pi+asin(y/r);
   end;
   Node(i,2)=r*cos(angle+delta_angle);
   Node(i,3)=r*sin(angle+delta_angle);
   Node(i,4)=z;
end;
```

VI SSTAN

```
% This rountine develops the SSTAN input file. It is wise to consult the SSTAN user's
%manual prior to running this routine to be sure the variables are input correctly. Also,
%be sure to place the loads on the correct nodes in order to analyze the system accurately.

% Formatting the Sstan input file
ln1=lastnode1(1)+1;
ln2=lastnode2(1);
NJT=mnodes(1);
NJT2=ln2;
NTE=2;
NE=melements(1);
NE2=melements2(1);
NF=1;
NL=NJT;
NL2=NJT2;
NM=NE;
%NM2=NE2-NE;
NM2=NE2;
NP=1;
NPB=2;
MID=1;
numbolt=size(nbolt);
L2=mnodes(1)/2+1;
% Load on 4 bolt square pattern
n_load=Element(NE/n+c*(cp+1)+(Cbplate-1)*c,5);
%check_node=Element(c*(cp+1)+1,4)
H1=Thickness_of_base_plate;
H2=Thickness_of_pipe;
```

```
%H2=.28
fprintf(fn,'Run 1\n');
fprintf(fn,'%1.0f %1.0f %1.0f\n',l_nodeb(1),NTE,NLC);
fprintf(fn,':\n');
fprintf(fn,'COORDINATES\n');
for i=1:l_nodeb(1);
   fprintf(fn,'%1.0f x=%6.3f y=%6.3f
z=%6.3f\n',Node(i,1),Node(i,2),Node(i,3),Node(i,4));
end;
fprintf(fn,':\n');
fprintf(fn,'BOUNDARY\n');
fprintf(fn,'%1.0f %1.0f DOF=r r r r r r\n',NF,l_nodeb(1));
for i=l_nodeb(1)-n:l_nodeb;
   fprintf(fn,'%1.0f DOF=f f f f f f\n',i);
end;
fprintf(fn,':\n');
fprintf(fn,'SHELL\n');
fprintf(fn,'%1.0f %1.0f\n',NM2,NP);
fprintf(fn,'%1.0f E=%1.0f U=%4.2f\n',MID,E,U);
for i=1:NE;
   fprintf(fn,'%1.0f
Q=%1.0f,%1.0f,%1.0f,%1.0f,M=%1.0f,H=%1.3f\n',Element(i,1),Element(i,2),Element(i,
3),Element(i,4),Element(i,5),MID,H1);
end;
for i=NE+1:NE2;
   fprintf(fn,'%1.0f
Q=%1.0f,%1.0f,%1.0f,%1.0f,M=%1.0f,H=%1.3f\n',Element(i,1),Element(i,2),Element(i,
3),Element(i,4),Element(i,5),MID,H2);
end;
fprintf(fn,':\n');


fprintf(fn,'BEAM\n');
fprintf(fn,'%1.0f %1.0f\n',NMB,NPB);
fprintf(fn,'%1.0f I=%2.4f,%2.4f J=%2.4f A=%4.4f,%4.4f,%4.4f
E=%1.0f\n',1,I21,I31,J1,A1,AS21,AS31,E);
fprintf(fn,'%1.0f I=%2.4f,%2.4f J=%2.4f A=%4.5f,%4.4f,%4.4f
E=%1.0f\n',2,I22,I32,J2,A2,AS22,AS32,E);
for i=1:numbolt(1);
   fprintf(fn,'%4.0f,%4.0f,%4.0f,%4.0f,M=%1.0f\n',bolt(i,1),bolt(i,2),bolt(i,3),bolt(i,4),1);
end;
for i=numbolt(1)+1:NMB;
   fprintf(fn,'%4.0f,%4.0f,%4.0f,%4.0f,M=%1.0f\n',bolt(i,1),bolt(i,2),bolt(i,3),bolt(i,4),2);
end;
fprintf(fn,':\n');
```

```
fprintf(fn,'LOADS\n');
fprintf(fn,'%1.0f %1.0f %1.0f L=%6.4f
F=%6.4f,%6.4f,%6.4f,%6.4f,%6.4f,%6.4f\n',n_load1,n_load2,inc
,LC,FX,FY,FZ,MX,MY,MZ);
fprintf(fn,':\n');
```

APPENDIX B
EXAMPLE SSTAN INPUT FILE

```
Run 1
979 2 1
:
COORDINATES
1 x= 4.162 y= 2.403 z= 0.000
2 x= 3.398 y= 3.398 z= 0.000
3 x= 2.403 y= 4.162 z= 0.000

965 x= 4.806 y= 0.000 z=72.000
966 x= 4.642 y= 1.244 z=72.000
967 x= 3.125 y= 5.413 z= 0.000
968 x=-3.125 y= 5.413 z= 0.000
969 x=-6.250 y= 0.000 z= 0.000
970 x=-3.125 y=-5.413 z= 0.000
971 x= 3.125 y=-5.413 z= 0.000
972 x= 6.250 y= 0.000 z= 0.000
973 x= 3.125 y= 5.413 z=-1.500
974 x=-3.125 y= 5.413 z=-1.500
975 x=-6.250 y= 0.000 z=-1.500
976 x=-3.125 y=-5.413 z=-1.500
977 x= 3.125 y=-5.413 z=-1.500
978 x= 6.250 y= 0.000 z=-1.500
979 x= 0.000 y= 0.000 z=-1.500
:
BOUNDARY
1 979 DOF=r r r r r r
973 DOF=f f f f f f
974 DOF=f f f f f f
975 DOF=f f f f f f
976 DOF=f f f f f f
977 DOF=f f f f f f
978 DOF=f f f f f f
979 DOF=f f f f f f
:
SHELL
912 1
1 E=29000 U=0.30
```

```
1 Q=1,2,26,41,M=1,H=1.500
2 Q=2,3,41,43,M=1,H=1.500
3 Q=3,4,43,45,M=1,H=1.500

910 Q=940,941,964,965,M=1,H=0.194
911 Q=941,942,965,966,M=1,H=0.194
912 Q=942,919,966,943,M=1,H=0.194
:
BEAM
78 2
1 I=0.516,0.516 J=1.032 A=2.002,22.6,22.6 E=29000
2 I=0.00516,0.00516 J=0.01033 A=1000.00000,0.226,0.226 E=29000
 913,  53, 967, 979,M=1
 914,  54, 967, 979,M=1
 915,  55, 967, 979,M=1
 916,  56, 967, 979,M=1

 988, 970, 976, 979,M=2
 989, 971, 977, 979,M=2
 990, 972, 978, 979,M=2
:
LOADS
945 965 4 L=1.0000 F=0.0000,0.1667,0.0000,0.0000,0.0000,0.0000
:
```

APPENDIX C

EXAMPLE SSTAN OUTPUT FILE

```
**********************************************************
        SSTAN  -  Simple Structural Analysis Program
  Copyright 1995  By  Dr. Marc Hoit, University of Florida
        Built in File Compression By Gary Consolazio
          Nodal Renumbering using the PFM algorithm
              Version 4.21     November 5, 1997

**********************************************************

 Run 1
 NUMBER OF JOINTS                        =  708
 NUMBER OF DIFFERENT ELEMENT TYPES       =    1
 NUMBER OF LOAD CONDITIONS               =    1
 NUMBER OF LOAD COMBINATIONS             =    0
 TOLERANCE FOR NONLINEAR SOLUTION        =  .0100
 Truss has Non-Compression/Tension       =  NO
 Frames/Beams Include P-Delta Effects    =  NO
 Sequential Loads Active                 =  NO
            NEURAL NETWORK RENUMBERING OUTPUT:
```

*** PRINT OF FINAL DISPLACEMENTS ***
DISPLACEMENTS FOR LOAD CONDITION 1

NODE	X	Y	Z	XX	YY	ZZ
1	.12790E-03	.76185E-04	-.71176E-02	.88707E-03	-.22996E-02	-.88618E-04
2	.47223E-04	.92771E-04	-.40235E-02	.20961E-02	-.42515E-03	-.21673E-04
3	-.44592E-04	.44605E-04	-.70879E-08	.13196E-02	.13201E-02	-.91077E-04
4	-.92777E-04	-.47242E-04	.40233E-02	-.42450E-03	.20962E-02	-.21704E-04
5	-.76201E-04	-.12791E-03	.71176E-02	-.22999E-02	.88754E-03	-.88528E-04
6	-.12545E-04	-.13640E-03	.84840E-02	-.33441E-02	-.20339E-02	-.32453E-03
7	.58226E-04	-.58233E-04	.86897E-02	-.43395E-02	-.43401E-02	-.10331E-06
8	.13641E-03	12525E-04	.84836E-02	-.20353E-02	-.33450E-02	.32455E-03
9	.12790E-03	.76185E-04	.71176E-02	.88707E-03	-.22996E-02	.88618E-04
10	.47223E-04	.92771E-04	.40235E-02	.20961E-02	-.42515E-03	.21673E-04
11	-.44592E-04	.44605E-04	.70879E-08	.13196E-02	.13201E-02	.91077E-04
12	-.92777E-04	-.47242E-04	-.40233E-02	-.42450E-03	.20962E-02	.21704E-04
13	-.76201E-04	-.12791E-03	-.71176E-02	-.22999E-02	.88754E-03	.88528E-04
14	-.12545E-04	-.13640E-03	-.84840E-02	-.33441E-02	-.20339E-02	.32453E-03

15 .58226E-04 -.58233E-04 -.86897E-02 -.43395E-02 -.43401E-02 .10331E-06

700 .47920E+00 -.47945E+00 .33501E-01 .78064E-02 .59073E-02 -.49414E-03
701 .47863E+00 -.47931E+00 .25605E-01 .60771E-02 .62795E-02 -.13718E-03
702 .47869E+00 -.47929E+00 .13845E-01 .62273E-02 .62909E-02 .22385E-03
703 .47905E+00 -.47905E+00 .41783E-09 .62531E-02 .62531E-02 .33540E-03
704 .47929E+00 -.47869E+00 -.13845E-01 .62909E-02 .62274E-02 .22385E-03
705 .47931E+00 -.47863E+00 -.25605E-01 .62795E-02 .60771E-02 -.13718E-03
706 .47945E+00 -.47920E+00 -.33501E-01 .59073E-02 .78064E-02 -.49414E-03
707 .48003E+00 -.48003E+00 -.36297E-01 .66495E-02 .66495E-02 .27605E-08
708 .47920E+00 -.47945E+00 -.33501E-01 .78064E-02 .59073E-02 .49414E-03

-------- PLANE/PLATE/SHELL STRESS RESULTS --------

------- ELEMENTS ARE IN THE X-Y PLANE ------

*** ELEMENTS ARE PLANE STRESS ***

EL#	LD#	PNT#	SX	SY	SXY		
			MX	MY	MXY	SXZ	SYZ
1	1	1	-.1604E+01	.4496E+00	.4711E+00		
		2	-.2552E+00	.1077E+01	.9902E+00		
		31	-.3293E+00	.8293E+00	.9005E+00		
		26	-.1574E+01	.2504E+00	.4212E+00		
		1	.1900E+00	.2580E+01	-.1267E-01	.1873E+01	-.5000E+01
		2	.1080E+01	.3004E+01	.3490E+00	.1873E+01	-.5000E+01
		31	.1028E+01	.2829E+01	.2900E+00	.1873E+01	-.5000E+01
		26	.2062E+00	.2438E+01	-.4389E-01	.1873E+01	-.5000E+01
2	1	2	-.2073E+01	.5965E+00	-.4866E-01		
		3	-.5338E+00	.1804E+01	.6828E+00		
		46	-.4967E+00	.1571E+01	.6226E+00		
		31	-.1918E+01	.4561E+00	-.5266E-01		
		2	-.4769E+00	.9470E+00	.1179E-01	.3785E+01	-.4366E+01
		3	-.1261E+00	.1425E+01	.2795E+00	.3785E+01	-.4366E+01
		46	-.1456E+00	.1297E+01	.2815E+00	.3785E+01	-.4366E+01
		31	-.4695E+00	.8557E+00	.3439E-01	.3785E+01	-.4366E+01
3	1	3	-.1805E+01	.5343E+00	-.6832E+00		
		4	-.5967E+00	.2072E+01	.4853E-01		
		48	-.4559E+00	.1917E+01	.5234E-01		
		46	-.1571E+01	.4975E+00	-.6231E+00		
		3	-.1424E+01	.1253E+00	-.2794E+00	.4368E+01	-.3785E+01
		4	-.9464E+00	.4765E+00	-.1195E-01	.4368E+01	-.3785E+01
		48	-.8554E+00	.4689E+00	-.3444E-01	.4368E+01	-.3785E+01
		46	-.1296E+01	.1448E+00	-.2813E+00	.4368E+01	-.3785E+01
4	1	4	-.1076E+01	.2556E+00	-.9904E+00		

```
          5 -.4496E+00  .1603E+01 -.4711E+00
        107 -.2503E+00  .1573E+01 -.4214E+00
         48 -.8287E+00  .3299E+00 -.9007E+00
          4 -.3004E+01 -.1080E+01 -.3493E+00  .4997E+01 -.1872E+01
          5 -.2580E+01 -.1888E+00  .1096E-01  .4997E+01 -.1872E+01
        107 -.2439E+01 -.2053E+00  .4238E-01  .4997E+01 -.1872E+01
         48 -.2830E+01 -.1028E+01 -.2902E+00  .4997E+01 -.1872E+01
  5   1 26 -.1377E+01  .2918E+00  .3978E+00
         31 -.2632E+00  .8258E+00  .8578E+00
         41 -.2705E+00  .8013E+00  .8497E+00
         36 -.1375E+01  .2719E+00  .3936E+00
         26 -.3606E+00  .2571E+01  .4929E+00  .1340E+01 -.2973E+01
         31  .1022E+01  .3146E+01  .8964E+00  .1340E+01 -.2973E+01
         41  .1017E+01  .3126E+01  .8861E+00  .1340E+01 -.2973E+01
         36 -.3547E+00  .2556E+01  .4860E+00  .1340E+01 -.2973E+01

670   1 690 -.6443E+00 -.1045E+00  .6902E+00
        691 -.7274E+00 -.2269E+00  .7419E+00
        707 -.9359E-01 -.7912E+00  .5145E+00
        706 -.1054E-01 -.6689E+00  .4628E+00
        690 -.3184E-02 -.4250E-02 -.3142E-03  .2404E-01  .1595E-01
        691 -.4030E-02 -.3342E-02  .3027E-04  .2404E-01  .1595E-01
        707  .2023E-01  .1293E-01  .1019E-01  .2404E-01  .1595E-01
        706  .2107E-01  .1203E-01  .9845E-02  .2404E-01  .1595E-01
671   1 691 -.2269E+00 -.7274E+00  .7419E+00
        692 -.1046E+00 -.6443E+00  .6902E+00
        708 -.6689E+00 -.1054E-01  .4628E+00
        707 -.7912E+00 -.9359E-01  .5145E+00
        691 -.3342E-02 -.4030E-02  .3029E-04 -.1595E-01 -.2404E-01
        692 -.4250E-02 -.3183E-02 -.3142E-03 -.1595E-01 -.2404E-01
        708  .1203E-01  .2107E-01  .9845E-02 -.1595E-01 -.2404E-01
        707  .1293E-01  .2023E-01  .1019E-01 -.1595E-01 -.2404E-01
672   1 692 -.4851E+00 -.3221E+00  .1160E+01
        677 -.1966E+00 -.2257E+00  .1121E+01
        693 -.6655E+00  .2045E+00  .8026E-02
        708 -.9541E+00  .1081E+00  .4684E-01
        692  .3516E-02  .6079E-02  .9005E-05 -.1488E-02 -.7312E-02
        677  .3791E-02  .5774E-02  .7312E-03 -.1488E-02 -.7312E-02
        693 -.4585E-02 -.1933E-01 -.2628E-02 -.1488E-02 -.7312E-02
        708 -.4859E-02 -.1903E-01 -.3350E-02 -.1488E-02 -.7312E-02
```

LIST OF REFERENCES

AISC Manual of Steel Construction Load & Resistance Factor Design, 2nd Edition, American Institute of Steel Construction, USA, 1995.

Billington, David P., Thin Shell Concrete Structures, McGraw-Hill Company, New York, 1965.

Collins, D. M., Cook, R. A., Klinger, R. E., and Polyzois, D., "Load-Deflection Behavior of Cast-in-Place and Retrofit Concrete Anchors Subjected to Static, Fatigue, and Impact Tensile Loads," Research Report No. 1126-1, Center for Transportation Research, University of Texas at Austin, Austin, Texas, 1989.

Cook, Robert D., Finite Element Modeling for Stress Analysis, John Wiley and Sons, Inc., New York, 1995.

Cook, R. A., Ellifritt, D. S.,Schmid, S. E., Adediran, A., and Beese, W., "Design Procedure for Annular Base Plates," Research Report No. 95-4, Engineering and Industrial Experiment Station, University of Florida, Gainesville, Florida, 1995.

Cook, R. A., and Klinger, R. E., "Behavior and Design of Ductile Multiple-Anchor Steel-to-Concrete Connections," Research Report No. 1126-3, Center for Transportation Research, University of Texas at Austin, Austin, Texas, 1989.

Cowper, G. R., "The Shear Coefficient in Timoshenko's Beam Theory," Journal of Applied Mechanics, June, 1966, pp 335-340.

DeWolf, John T., Design of Column Base Plates, American Institute of Steel Construction, Chicago, Illinois, 1991.

Hoit, M.I., Computer Assisted Structural Analysis and Modeling, Prentice Hall, New Jersey, 1995.

Langhaar, Henry L., Dimensional Analysis and Theory of Models, Robert E. Krieger Publishing Company, Malabar, Florida, 1951.

Standard Specifications for Structural Supports for Highway Signs, Luminaires, and Traffic Signals, AASHTO, Washington, D.C., 1994.

Timoshenko, S. and Woinowsky-Krieger, S., Theory of Plates and Shells, McGraw-Hill Book Company, New York, 1969.

Ugural, A. C., Stresses in Plates and Shells, McGraw-Hill Book Company, New York, 1981.

Wahl, A. M., and Lobo, G. Jr., "Stresses and Deflections in Flat Circular Plates with Central Holes," Transactions of the Society of Mechanical Engineers, APM-52-3, 1933, pp 29-43.

Young, Warren C., Roark's Formulas for Stress and Strain, McGraw-Hill Book Company, New York, 1989.